This is a non-peer-reviewed preprint submitted to EarthArXiv.

Variable methane–arsenic interactions in groundwater of Northern Bangladesh revealed by stable isotopes and geochemical analyses

Kai Ernst[a], Charlotte Stirn[a], Martin Maier[a,b], Moritz Schroll[a], David A. Polya[c], Frank Keppler[a,b*]

[a]Institute of Earth Sciences, Heidelberg University, Im Neuenheimer Feld 234–236, 69120 Heidelberg, Germany

[b]Heidelberg Center for the Environment (HCE), Heidelberg University, D-69120 Heidelberg, Germany

[c]Department of Earth and Environmental Sciences and Williamson Research Centre for Molecular Environmental Science, The University of Manchester, Williamson Building, Oxford Road, Manchester, M13 9PL, UK

**Correspondence to*: Frank Keppler (frank.keppler@geow.uni-heidelberg.de)

Key words

Arsenic mobilisation, groundwater contamination, stable isotopes, iron oxides, methane formation and oxidation, Bangladesh

Abstract

The reductive dissolution of arsenic (As)-bearing Fe(III) (hydr)oxides is widely regarded as the primary mechanism driving As mobilisation into groundwater in the aquifers of Bangladesh. Recently, methane (CH_4) has been proposed as a potentially important electron donor in this process, with CH_4 oxidation by methanotrophic bacteria facilitating Fe(III) reduction and subsequent As release. However, the role of CH_4 in As mobilisation remains poorly constrained, particularly regarding the origin, prevalence, and vertical distribution of CH_4 production and oxidation. Here, we present compelling field-based evidence for As mobilisation linked to CH_4 cycling, based on a comprehensive, depth-resolved dataset from four groundwater wells in northern Bangladesh. This includes isotopic measurements of $\delta^{13}C_{VPDB}$-CH_4, $\delta^{2}H_{SMOW}$-CH_4 , $\delta^{13}C_{VPDB}$-CO_2 as well as of various other hydrogeochemical parameters. Two of the wells exhibited high dissolved As

concentrations, with depth-specific profiles showing significant correlations between As, Fe(II), and CH_4. In particular, isotopic signatures of CH_4 and CO_2 revealed that CH_4 formation and oxidation processes were closely associated with zones of elevated As. In contrast, the other two wells showed relatively low As and Fe(II) concentrations and no clear evidence of CH_4-driven biogeochemical activity. Our findings suggest that, depending on site-specific hydro-biogeochemical conditions, Fe(III) (hydr)oxide reduction coupled to CH_4 oxidation may substantially contribute to As mobilisation in Bangladeshi aquifers and potentially in other As-impacted regions worldwide.

1 Introduction

In Bangladesh, more than 52 million people consume potentially toxic groundwater with dissolved arsenic (As) concentrations above the World Health Organization provisional guidevalue for drinking water of 10 $\mu g\ l^{-1}$ (Bangladesh Bureau of Statistics (BBS) and UNICEF Bangladesh, 2015). The long-term intake of As via drinking water may have toxicological effects, affecting many cellular processes and organ functions (Abdul et al., 2015) and so may lead to a variety of diseases such as chronic As poisoning, or increased risks of various forms of cancer (Smith & Steinmaus, 2009; Volanis et al., 2010) and cardiovascular disease (Xu et al., 2020; Wu et al., 2021). Although research on As-contamination in South Asia and Bangladesh in particular has spanned more than three decades (e.g. Dhar et al., 1997; BGS and DPHE, 2001; Harvey et al., 2002, Islam et al., 2004, Neumann et al, 2010; Neumann et al., 2014; Bhattacharya et al., 2017; Wu et al., 2023), the underlying biogeochemical processes leading to enhanced dissolved As-concentrations in the groundwater are still subject to debate.

Iron(III)-oxides, -hydroxides and -oxy-hydroxides (collectively termed hereafter as Fe(III) (hydr)oxides) are the most important As-containing minerals in the aquifers of Bangladesh, because of their ability to adsorb dissolved As on their surface, resulting in the formation of stable surface complexes (Swartz et al., 2004). Therefore, the primary cause of the As-contamination in these reducing aquifers is the dissolution of these Fe(III) (hydr)oxides under reducing conditions (Islam et al., 2004; Charlet & Polya, 2006; Smedley & Kinniburgh, 2002), which makes it key to understand the identity and the source of the electron donors that drive the reduction process (Moore et al., 2023). In general, the input of organic carbon, the subsequent dissolution and the oxidative degradation of dissolved organic carbon (DOC) fuels the microbial catalysed reduction of various electron acceptors including Fe(III) (hydr)oxides, resulting in a reducing redox

environment critical for the possibility of redox-driven As-mobilisation. Therefore, the interaction between the carbon cycle and As-mobilisation has been investigated intensively in recent years, clearly showing that the DOC in the aquifers originates from different anthropogenic and natural sources resulting in variable bioavailability for microbial degradation (Rowland et al., 2007). Moreover, different organic compounds have been identified to serve as electron donors for Fe(III) (hydr)oxide reduction and subsequent As-mobilisation (Glodowska et al., 2020).

However, under strong anoxic conditions, when all electron acceptors (e.g., Fe(III), SO_4^{2-}) besides CO_2 are reduced, it is methane (CH_4) formation that largely contributes to the carbon cycle and thus controls electron donor availability. Considering As-contamination, several studies demonstrated noticeable correlations between dissolved As, Fe(II) and CH_4, indicating a close relation between CH_4 availability, Fe(III) (hydro)xide reduction, and As-mobilisation (Harvey et al., 2002; Stopelli et al., 2021). Moreover, CH_4 is abundant in many As-contaminated aquifers worldwide (Liu et al., 2009; Sø et al., 2018). Although CH_4 for As-mobilisation has rarely been considered as the most important electron donor, especially in natural settings (Polya, et al., 2019), in recent years, researchers have started to investigate more closely the role of CH_4 as an electron donor driving the reductive dissolution of Fe(III) (hydr)oxides in As-contaminated aquifers (Glodowska et al., 2021; Stopelli et al., 2021). Furthermore, very recently Moore et al. (2023) critically reviewed the involvement of various electron donors including CH_4 on As-mobilisation and underlined the need for further research to understand this interaction in greater detail.

Aquifer CH_4 may be formed by methanogenic archaea (biogenic CH_4), or provided the abiotic thermocatalytic breakdown of complex organic molecules (thermogenic CH_4) (Stolper et al., 2014). In order to trace the role of CH_4 as an electron donor for As-mobilisation to these different CH_4 sources, it is important to distinguish thermogenic from biogenic CH_4 contributions, which are common in shallow anoxic aquifers (Beeman & Suflita, 1990; Kleikemper et al., 2005). In aquatic systems, including aquifers, biogenic CH_4 formation results from the development of strict reducing conditions (E_h < -200 mV) and the presence of small carbon precursor molecules, leading to methanogenesis by methanogenic archaea (Whiticar, 1999). The most common biological reaction pathways for methanogenic CH_4 formation are acetoclastic (Eq. 1) and hydrogenotrophic (Eq. 2) methanogenesis, carried out by different species of methanogenic archaea (Goevert & Conrad, 2009). Both equations should be considered as highly simplified representations of more complex biological formation pathways.

$$CH_3COOH \rightarrow CO_2 + CH_4 \quad (1)$$

$$CO_2 + 4H_2 \rightarrow 2H_2O + CH_4 \quad (2)$$

Once formed, dissolved CH_4 from either thermogenic and/or biogenic origin can migrate through the aquifer and be utilised by methanotrophic microorganisms as an electron donor in the course of CH_4 oxidation to CO_2, both under aerobic (aerobic methane oxidation) (Knittel & Boetius, 2009) and anaerobic (anaerobic methane oxidation) conditions (Dumont & Mureell, 2005). In many aquatic systems, especially in marine environments and under anoxic conditions, the electron acceptor sulphate (SO_4^{2-}) is abundant in high concentrations and for a long time it was assumed that CH_4 oxidation under anoxic conditions is mainly related to SO_4^{2-} reduction (Knittel & Boetius, 2009). However, in aquatic habitats characterised by low SO_4^{2-} concentrations, it has been demonstrated that CH_4 oxidation can also be coupled to the reduction of other electron acceptors, including Fe(III) (hydr)oxides, resulting in high dissolved Fe(II), carbon dioxide (CO_2) and subsequent As concentrations (Pienkowska et al., 2021).

Stable carbon and hydrogen isotope values of CH_4 (δ^{13}C-CH_4 and δ^{2}H-CH_4 respectively) and CO_2 (δ^{13}C-CO_2) in combination with Bernard ratios (the molar ratio between CH_4 and ethane and propane) have been applied to better identify the different CH_4 formation and oxidation pathways in the environment (Whiticar, 1999; Whiticar et al., 1986). However, until now, only few studies have applied this approach for gaining deeper understanding of the influence of CH_4 in As-prone aquifers.

Stopelli et al. (2021) used stable carbon isotopes measurements (δ^{13}C-CH_4, δ^{13}C-DOC, δ^{13}C-dissolved inorganic carbon = DIC) and demonstrated that all of anaerobic fermentation, hydrogenotrophic methanogenesis and anaerobic methanotrophy are important processes of the carbon cycle and influence dissolved As concentrations in an aquifer near Hanoi (Vietnam). Furthermore, in the same study area, CH_4 oxidation coupled to As-mobilisation has been characterised by laboratory investigations in incubated aquifer sediments using microbial analysis (Glodowska et al., 2021) and isotopically labelled CH_4 (Pienkowska et al., 2021). These CH_4 based investigations were all carried out in the same aquifer area (Red River Delta). It is difficult to directly apply these results to other geographical locations with As-contaminated aquifers such as Bangladesh, where hydraulic and hydrogeochemical conditions are different. For many sites in Bangladesh, the highest dissolved As concentrations are found in the upper 30 m of the aquifer indicating pronounced As-mobilisation in the upper sediment layers (Reza & Jean, 2012). Thus, it is relevant to characterise CH_4 cycling with high-resolution vertical profiles in order to identify at which depths CH_4 is formed and consumed within

As-prone aquifers (Moore et al. 2023). To the best of our knowledge, to date, there exists no study in Bangladesh that have characterised CH_4 cycling in As-contaminated aquifers using field based, high-resolution, depth-specific stable isotope measurements and comparison with various geochemical parameters.

In this study, we performed field-based investigations at four groundwater wells located at two sites in northeast and northwest Bangladesh using depth-specific groundwater and dissolved gas sampling. With this approach, we provide a vertical characterisation of CH_4 cycling using stable isotope values ($\delta^{13}C$-CH_4; $\delta^{2}H$-CH_4 and $\delta^{13}C$-CO_2) at high depth resolution and compare them with various geochemical data indicative of As-mobilisation. Please note that within this project we could not conduct any additional microbial analysis to further determine the microbial communities involved in CH_4 cycling.

2 Materials and Methods

2.1 Well characteristics

The well drillings took place in February of 2020 and was carried out using the "hand flapper method" (for details see Hornemann et al., 2004) with a 2'' drilling device to a depth of 50 m. During the drilling of the wells, the sediment was collected every 3.05 m and analysed by the biogeochemistry group from University Heidelberg (e.g., grain size; unpublished). A fully slotted, screened 2'' PVC pipe was installed in each borehole with minimal annulus backfill to allow sediment to collapse and avoid vertical mixing during the water sampling procedure.

The four groundwater wells are located in two different parts of Bangladesh (Fig. 1). Two of the wells are located in the northwest of Bangladesh at the Bera site in the district Pabna of the Rajshahi division about 150 km northeast of Dhaka. One of these wells (BB1, Latitude: 24.004109, Longitude: 89.647699) was built in Bera village, between a pond and a latrine and next to a water-bearing oxbow lake of the Brahmaputra River. The other well (BB2, Latitude: 24.004406, Longitude: 89.645164) was built about 250 m west of BB1 in an agricultural area. The other two wells are located in the northeast of Bangladesh at the Korgaon site in the district Habiganj of the Sylhet division about 80 km west-northwest of Dhaka. While one of these wells (KB1, Latitude: 24.004109, Longitude: 89.647699) was built in Korgaon village, surrounded by household ponds and a highly frequented latrine of a primary school, the other well (KB2, Latitude: 24.004406, Longitude: 89.645164) is located about 250 m north of KB1 in an agricultural area. Both agricultural areas, in which BB2 and KB2 are located, are used for rice cultivation.

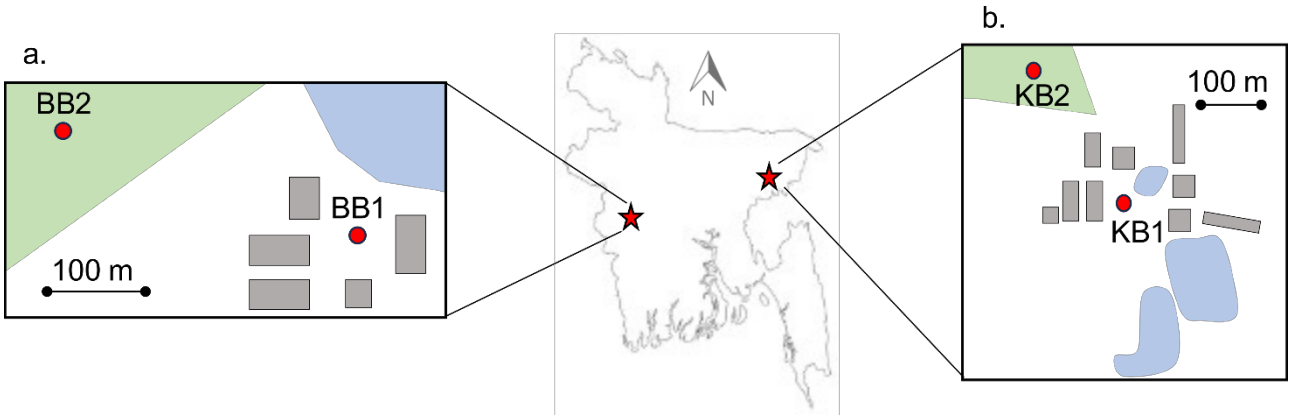

Fig 1. Map and schematic overview of the two sites and the groundwater wells within Bangladesh with a.: Bera site, in the district Pabna of Rajshahi division and b.: Korgaon site, in the district Habiganj of Sylhet division. Gray blocks represent houses in villages, green areas represent agricultural areas and blue areas show surface aquatic habitats such as an oxbow lake of the Brahmaputra or ponds in a. and b. respectively.

The two sites Bera and Korgaon have been intensely studied by Heidelberg University in previous years. Since Korgaon has been characterised by high dissolved As concentrations and Bera by rather low dissolved As concentrations in the previous investigations, these locations were chosen as being representative of contrasting relatively high As-aquifers and low As-aquifers. The local differences (urban vs. agriculture) of two wells within one site were chosen to investigate whether agricultural areas or villages alter the environmental conditions in the aquifers and consequently have an impact on As-mobilisation and CH_4 pathways in groundwater. Please note that no hydrological data concerning the groundwater flow direction could be obtained for the locations preventing interpretations of our results in relation to groundwater flow directions.

2.2 Sample collection

Sampling of the groundwater and the dissolved gases at the four wells in Bangladesh was carried out in May 2022. The procedure of sample collection was identical for every well. First an optical water level meter was used to determine the groundwater level. Second the groundwater was pre-pumped (all depths, each with a flow rate ~ 40 ml min^{-1}) for 30 min to achieve a full groundwater exchange within the well. Subsequently, depth-specific groundwater and dissolved gas sampling at ten different depths (2.5 m, 5 m, 7.5 m, 10 m, 12.5 m, 15 m, 17.5 m, 20 m, 25 m, 30 m) was conducted. Multilevel sampling was achieved through the installation of 10 extraction tubes according to the sampling depth. Laminar water flow was established by slowly extracting water with a set of five pumps (40 ml min^{-1}; 12V peristaltic liquid pump, TOPINCN) running

simultaneously. Please note that the groundwater levels at BB2 and KB2 were deeper than 2.5 m, so sampling at this depth was not possible.

From each specific depth, the groundwater was pumped through a gastight measurement unit containing four probes to determine *in-situ* the parameters pH and temperature (T; SenTix 940; WTW), electric conductivity (EC; TetraCon 925, WTW) and redox potential (E_H; SenTix ORP-TR900, WTW). Due to technical problems of the probe for measuring oxygen concentration (FDO 925; WTW) this parameter is omitted in the following evaluations. Redox potentials were measured in relation to an Ag/AgCl electrode and were therefore converted to redox potential relative to the standard hydrogen electrode (SHE).

After *in-situ* measurements were made, groundwater sampling was carried out using a 60 ml syringe (BD Plastikpak™; USA), which was connected to the tube by a three-way valve. For the analysis of dissolved ions and DIC, two 15 ml falcon tubes (Corning; USA) were filled with filtered groundwater (0.45 µm filter; Puradic FP; Whatman™; UK). One of the falcon tubes was previously acidified with 100 µl 6 M HCl for cation analysis, the other sample tube did not receive any pre-treatment and was used for anion analysis.

For depth specific gas sampling the headspace method was used (for details see Wilson et al., 1989). In brief, a 100 ml syringe (Monoject™; Switzerland) was filled with 60 ml groundwater and 40 ml of helium (He 5.0; Alphagaz™; France) was added via a three-port valve to create a headspace. The syringe was then vigorously shaken for 90 seconds to equilibrate the water and the headspace. Finally, the total headspace volume was extracted using another syringe and transferred into a pre-evacuated 12 ml sample vial (Exetainer®; Labco; UK).

2.3 Water analysis

The concentrations of dissolved As, Fe, phophorous (P) and other elements were analysed using an inductively coupled plasma optical emission spectrometer (ICP-OES 720; Agilent Technologies; USA). Each sample was measured by an autosampler as an internal triplet measurement (n = 3). The mean relative standard deviation (RSD) for each element indicated a mean measurement precision of better than 3.6 %. Quality control included analysing the reference materials SPS-SW2 (Batch 142), SPS-SW2 (Batch 117) and TMDA-61.3 and for which recovery rates were determined to be in the range of 100-106 % for all analysed elements.

The concentrations of anions were determined using ion chromatography (ICS-1100; Dionex; USA). Before measurement, each sample was filtered (Puradisc FP; inner diameter: 45 µm, Whatman™; UK). Analysis was carried out as single measurements. The reference material SPS-NUTR-WW1 batch 113 was

analysed for quality control with recovery rates in the range of 85-104 %. Long-term repeated analysis of this reference material yielded a measurement precision < 14 % for each element.

Concentrations of DIC and total carbon (TC) were determined using a TOC-analyzer (TOC-VCPH equipped with an ASI-V autosampler; Shimadzu; Japan). By measuring the total carbon- and total inorganic carbon concentration, the total organic carbon concentration was calculated by difference. Please note that all samples were filtered prior the measurement, therefore the results are reported as DIC and DOC.

2.4 Dissolved gas analysis

For the analysis of CH_4 mixing ratios between 100 parts per billion by volume (ppbv) to 50 parts per million by volume (ppmv), as well as mixing ratios of ethane (C_2H_6) and propane (C_3H_8), a gas chromatograph (GC; GC 6000 Vega Series 2; Carlo Erba Strumentazione; Italy) coupled to a flame ionisation detector (FID) was used. The GC system was equipped with a capillary column (J&W HP-AL/S; length: 30 m; inner diameter: 0.53 mm; thickness: 15 µm; Agilent Technologies; USA) with nitrogen as carrier gas (pressure: 150 kPa). For quantification purposes, the GC-FID was calibrated using several reference gases with different CH_4, C_2H_6 and C_3H_8 mixing ratios.

For the analysis of CO_2 mixing ratios and CH_4 mixing ratios exceeding 50 ppmv, a GC (GC-2010 Plus; Shimadzu; Japan) coupled to a barrier ionization detector (BID-2010 plus; Shimadzu; Japan) was used. The GC system was equipped with a stainless-steel packed column (ShinCarbon ST; 80/100 mesh; length: 2 m; inner diameter: 0.53 mm) with helium as carrier gas (Helium 6.0, Flowrate 50 ml min^{-1}; Alphagaz™; Germany). For quantification purposes, the GC-BID was calibrated using several reference gases in various dilution steps with different CH_4 and CO_2 mixing ratios. For quality control, one of the reference gases was measured periodically between the samples.

The dissolved CH_4 and CO_2 concentrations were calculated from the headspace mixing ratio by calculating the solubility constants according to Weiss (1970) with experimentally determined constants according to Yamamoto et al. (1976) and Weiss (1974) for CH_4 and CO_2, respectively.

For the analysis of $\delta^{13}C_{VPDB}$-CH_4 and $\delta^{2}H_{SMOW}$-CH_4 values an isotope ratio mass spectrometer (IRMS; DeltaPlus XL; ThermoFisher Scientific; USA) coupled to a GC (HP 6890N; Agilent Technologies; USA) via an interface (Combustion III; ThermoFisher Scientific; USA) with an oxidation and reduction reactor was used. Before entering the GC IRMS system, the sample was introduced via a cryogenic pre-concentration unit consisting of three cold traps cooled by liquid nitrogen in thermically isolated dewars. In the first cold trap (T:

-150 °C; stainless steel tube; diameter: 3.175 mm) CH_4 was separated from the sample matrix and enriched in the second (T: -130 °C; HayeSep D; divinylbenzene; stainless steel tube; diameter: 3.175 mm) and third cold trap (T: -196 °C; deactivated quartz capillary; length: 50 cm; inner diameter: 0.25 mm). By heating the third cold trap up to room temperature, CH_4 entered the GC which was equipped with a capillary column (type: ZB-5 ms; length: 30 m; internal diameter: 0.25 mm; film thickness: 1 µm). The following oxidation reactor (ceramic tube; length: 320 mm; inner diameter: 0.5 mm) was filled with O_2-activated Cu/Ni/Pt wires and operated at a reactor temperature of 960 °C for stable carbon isotope analysis. The reduction reactor (ceramic tube; length: 320 mm; inner diameter: 1 mm) was working at 1450 °C for high temperature conversion (HTC) for stable hydrogen isotope analysis. The $\delta^{13}C_{VPDB}$-CH_4 and $\delta^{2}H_{SMOW}$-CH_4 values were corrected using two reference standards (Isometric instruments; Canada) with $\delta^{13}C_{VPDB}$-CH_4 values of −42.32 ‰ and −66.35 ‰ and $\delta^{2}H_{SMOW}$-CH_4 values of −190.6 ‰ and −149.9 ‰, respectively, that were calibrated against International Atomic Energy Agency (IAEA) and National Institute of Standards and Technology (NIST) reference substances. The measured isotope ratios were normalised according to Paul et al. (2007).

For analyses of $\delta^{13}C_{VPDB}$-CO_2 values an IRMS (MAT 253 PlusTM; Thermo Fisher Scientific; USA) coupled to a GC (HP 6890N GC; Agilent Technologies; USA) via an interface (GC Combustion III Interface; ThermoQuest Finnigan; USA) was used. Samples entered the GC via an autosampler (A200S; CTC Analytics; Swiss) and split injection (1:10) The GC was equipped with a capillary column (CP-PoraPLOT Q; length: 27.5 m; inner diameter: 0.25 mm; film thickness: 0 µm; Varian; USA). Samples were measured as triplicates, normalised according to Paul et al (2007) and corrected using a reference gas with a $\delta^{13}C_{VPDB}$-CO_2 value of -35.71 ‰. Furthermore, measurement errors relating to isobaric isotopologues were corrected according to Craig (1957).

2.5 Ionic balance

As a further quality control measure, ion balance was determined from the sum of major cationic and anionic charge according to Appelo & Postma (2005) (Eq. 3).

$$I = \frac{\sum m_c Z_c \mp \sum m_a Z_a}{\sum m_c Z_c - \sum m_a Z_a} \times 100 \quad (3)$$

where m and Z are the molar concentration and formal ionic charge respectively of the subscripted cationic (c) or anionic (a) species.

The majority of samples showed an ion balance of better than ± 5 %, however17 samples deviated in their ionic balance by at least ±5 %, albeit with the vast majority showing a deviation of +5 % and thus a small cation excess. Precipitation of dissolved main anions might explain the relatively low anion concentrations and the deviations in the ionic balances. In particular, many samples for anion analysis showed a notable brown coloration, indicating that important main anions such as HCO_3^- precipitated with Fe(II) forming iron carbonates ($FeCO_3$). Since the anion sample in contrast to the cation sample, was not stabilized with acid, the precipitated minerals were probably retained during the filter process and thus, the filter-retained HCO_3^- anions are missing from the measurement and ultimately from the anion sum.

2.6 Stable isotope nomenclature

To characterise the CH_4 cycling in the aquifer stable carbon and hydrogen isotope values of CH_4 and CO_2 were measured. Ratios (R) of the stable carbon ($^{13}C/^{12}C$) and hydrogen isotopes ($^{2}H/^{1}H$) are given in the conventional δ-notation versus an international standard material (Eq. 4).

$$\delta_{sample} = \left(\frac{R_{sample}}{R_{standard}}\right) - 1 \quad (4)$$

Where the international standard reference material for stable carbon isotopes is Vienna PeeDee Belemnite (VPDB) and for hydrogen isotopes is Vienna Standard Mean Ocean Water (V-SMOW). δ-values are given in per mil (‰) as $\delta^{13}C_{VPDB}$-CO_2, $\delta^{13}C_{VPDB}$-CH_4 and $\delta^{2}H_{SMOW}$-CH_4.

Kinetic isotope fractionation effects are of particular relevance in this work, e.g., during CH_4 oxidation. The kinetic isotope fractionation results from the mass dependent stability of the bonds of light and heavy isotopes. The cleavage of a bond with heavy isotopes requires a higher activation energy and a slower reaction rate compared to bond with a light isotope (Thullner et al., 2013). As a result, the reaction rates in biochemical, including microbial reactions, are higher for light isotopes such as ^{12}C and ^{1}H, resulting in a fractionation and residual enrichment of heavy isotopes ^{13}C and ^{2}H (Holler, 2010).

2.7 Statistics

Most analysed parameters were measured as three independent replicates (n = 3) and are reported as arithmetic mean ($\bar{x}$) and related standard deviations (SD). Please note that the standard deviation for the selected scaling for some parameters is too small to be seen in the diagram. The arithmetic means, their standard deviations as well as the linear regression analyses of different parameters were calculated using Microsoft Excel (Microsoft Excel for Office 365 MSO). The coefficient of determination (r) was calculated to evaluate how differences in one variable can be explained by a difference in a second variable and is interpreted

as in Akoglu (2018). Please note, that in adherence to the American Statistical Association recommendations, this study refrained from employing the term "statistically significant" (Wasserstein et al., 2019). Thus, the analysis of the data used in within this study did not rely exclusively on statistical parameters such as the p-value for interpreting the results.

3. Results

3.1 Depth-specific in-situ parameters of the four wells

In this section we present the measured in-situ parameters of the groundwater including temperature-, pH-, EC- and E_H-values. Please note that data on O_2-saturation are not inlcuded due to technical issues with the probe encountered during the field campaign.

While the groundwater temperature in BB1 showed little variation between 27 °C at a depth of 15 m and 27.6 °C at 5 m and 7.5 m (average mean of the groundwater profile: $\bar{x}$ = 27.3 ± 0.2 °C), the temperatures in BB2 were generally slightly warmer and ranging between 29.1 °C at 5 m and 32.8 °C in 30 m ($\bar{x}$ = 30.6 ± 1.1 °C) (Table 1). The pH values of groundwater in both wells varied only slightly within the neutral pH range, averaging $\bar{x}$ = 6.83 ± <0.1 in BB1 and a slightly higher $\bar{x}$ = 7.13 ± <0.1 in BB2. In BB1, the EC values ranged between 562 µS cm^{-1} at 17.5 m depth and 612 µS cm^{-1} at 12.5 m depth ($\bar{x}$ = 594 ± 15 µS cm^{-1}), while in BB2 they were slightly lower and ranged between 494 µS cm^{-1} at 2.5 m and 557 µS cm^{-1} in 10 m ($\bar{x}$ = 547 ± 18 µS cm^{-1}). Noticeable differences between the two wells were observed in the E_h values, which ranged between 133 mV at 17.5 m depth to 159 mV at 5 m depth ($\bar{x}$ = 144 ± 9 mV) and were therefore substantially lower than in BB2, which showed a range between 265 mV in 5 m and 380 in 30 m depth ($\bar{x}$ = 339 ± 36 mV).

Table 1. Depth-specific in-situ parameters (T, pH-, EC- and E_H-values) of the wells BB1 and BB2 at the Bera Site, NW-Bangladesh.

	BB1				BB2			
depth (m)	T (°C)	E_h (mV)	EC (µS cm^{-1})	pH (/)	T (°C)	E_h (mV)	EC (µS cm^{-1})	pH (/)
2.5	-	-	-	-	29.2	342	494	7.17
5	27.6	159	601	6.84	29.1	265	553	7.13
7.5	27.6	154	608	6.84	29.8	297	555	7.13
10	27.4	150	608	6.84	30.2	318	557	7.15
12.5	27.1	150	612	6.85	30.5	324	554	7.11
15	27.0	139	595	6.83	30.3	365	549	7.13
17.5	27.1	133	562	6.82	31.7	370	552	7.13
20	27.5	135	583	6.82	31.5	363	550	7.12
25	27.3	139	588	6.83	31.0	370	551	7.10
30	27.1	137	593	6.83	32.8	380	553	7.13

The groundwater temperatures in KB1 were generally slightly colder than in KB2 and both showed small variations, with arithmetic means of 26.6 ± 0.2 °C and 28.1 ± 0.4 °C respectively (Table 2). In both wells, pH values were in a neutral pH range and varied between 6.26 at 5 m and 7.5 m and 6.43 at 30 m in KB1 ($\bar{x}$ = 6.36 ± <0.1) and between 6.26 at 5 m and 6.64 at 30 m in KB2 ($\bar{x}$ = 6.42 ± 0.1). The EC values in KB1 ranged from 1173 µS cm^{-1} at 5 m to 1706 µS cm^{-1} at 30 m ($\bar{x}$ = 1454 ± 184 µS cm^{-1}) and were much higher than in KB2, where values ranged between 281 µS cm^{-1} at 2.5 m and 351 µS cm^{-1} at 10 m ($\bar{x}$ = 315 ± 21 µS cm^{-1}). While the E_H values in KB1 ranged between 111 mV at 25 m and 129 mV at 7.5 m ($\bar{x}$ = 119 ± 6 mV), the E_H values in KB2 were slightly higher between 124 mV at 10 m and 157 mV at 20 m ($\bar{x}$ = 141 ± 11 mV).

Table 2. Depth-specific in-situ parameters of the wells KB1 and KB2 at the Korgaon Site, NE-Bangladesh.

	KB1				KB2			
depth (m)	T (°C)	E_h (mV)	EC (µS cm^{-1})	pH (/)	T (°C)	E_h (mV)	EC (µS cm^{-1})	pH (/)
2.5	-	-	-	-	28.0	147	281	6.28
5	26.7	127	1173	6.26	27.6	136	311	6.26
7.5	26.3	129	1166	6.26	27.8	128	316	6.37
10	26.3	121	1372	6.34	27.9	124	351	6.46
12.5	26.3	112	1438	6.36	28.5	135	327	6.39
15	26.8	119	1455	6.37	28.4	138	316	6.39
17.5	26.7	115	1489	6.39	28.5	150	308	6.43
20	27.0	113	1619	6.39	27.7	157	294	6.52
25	26.8	111	1666	6.40	28.4	156	299	6.46
30	26.7	123	1706	6.43	28.6	141	346	6.64

3.2 Bera site – vertical profiles of geological, geochemical and stable isotope parameters

Before water sampling, the groundwater level in BB1 was 3.54 m below ground level (Figs. 2a-h). The sediment analysis at BB1 showed grain sizes in the range of silt up to 12.2 m and in the following grain sizes in the range of sand up to 35 m. Dissolved As concentrations showed only small variations until depths of up to 15 m ($\bar{x}$ = 24.5 ± 7.6 µg l^{-1}), followed by a strong increase to the maximum of 39.6 µg l^{-1} at 20 m and a decrease in the lower depths. Dissolved Fe(II) concentrations ($\bar{x}$ = 2.8 ± 0.9 mg l^{-1}) were similar to that of the dissolved As concentrations, especially with regard to the increase from 15 m to the maximum of 5.3 mg l^{-1} at 20 m, and they show a strong positive linear correlation with a coefficient of correlation (r) of 0.86 ($p < 0.01$). Also, dissolved CH_4 ($\bar{x}$ = 0.7 ± 0.3 mg l^{-1}) and phosphate (PO_4^{3-}) concentrations ($\bar{x}$ = 519 ± 188 µg l^{-1}) showed similar depth-specific trends and relationships to the dissolved As concentrations with a moderate positive linear correlation (r = 0.57, p = 0.11) and a strong positive linear correlation (r = 0.99, $p < 0.001$) for CH_4 and PO_4^{3-}, respectively. The DOC concentrations ($\bar{x}$ = 28.6 ± 10.0 mg l^{-1}) were highest between 15 m to 25 m and showed a strong negative linear correlation with DIC concentrations ($\bar{x}$ = 71.8 ± 3.0 mg l^{-1}) with r = -0.83 (p

321 < 0.006). Dissolved CO_2 concentrations ($\bar{x}$ = 50.4 ± 1.3 mg l^{-1}) showed a weak positive correlation with
322 dissolved CH_4 concentrations (r < 0.02, p = 0.95).

323 The $\delta^{13}C_{VPDB}$-CH_4 values ($\bar{x}$ = −70.4 ± 7.3 ‰) and the $\delta^{2}H_{SMOW}$-CH_4 values ($\bar{x}$ = −182 ± 15.9 ‰) both
324 showed their minimum values at a depth of 20 m with −64.8 ‰ and −171 ‰, respectively. This corresponds
325 to the depth with the highest dissolved As concentration. Also, $\delta^{13}C_{VPDB}$-CH_4 and $\delta^{2}H_{SMOW}$-CH_4 values showed
326 a similar depth-specific trend towards more negative values with depth and a strong positive linear correlation
327 (r = 0.91, p < 0.001). $\delta^{13}C_{VPDB}$-CO_2 ($\bar{x}$ = −16.5 ± 0.7 ‰) were approximately constant in the profile and showed
328 a weak negative linear correlation with $\delta^{13}C_{VPDB}$-CH_4 values (r = −0.14, p = 0.73).

329 The groundwater level in BB2 was 2.47 m below ground level before water sampling (Figs. 2i-p). The
330 sediment analysis at BB2 showed grain sizes in the range of silt up to 3 m and in the following grain sizes in
331 the range of sand up to 35 m. Dissolved As concentrations were below the detection limit at all sampled depths
332 and are therefore reported as < 10 µg l^{-1}. Dissolved Fe(II) ($\bar{x}$ = 0.07 ± 0.05 mg l^{-1}) and dissolved CH_4
333 concentrations ($\bar{x}$ = 0.01 ± 0.003 mg l^{-1}) were relatively low compared with BB1 and showed similar depth-
334 specific trends, including an increase between 2.5 m to 5 m and in the lower depths a trend towards lower
335 concentrations until a depth of 30 m. Dissolved PO_4^{3-} concentrations were below the detection limit at seven
336 sampled depths (2.5 m, 7.5 m, 15m to 30m) and are therefore reported as < 50 µg l^{-1}. In the remaining depths
337 the dissolved PO_4^{3-} concentrations were lower than at BB1 ($\bar{x}$ = 52 ± 1 µg l^{-1}). DOC ($\bar{x}$ = 31.7 ± 6.5 mg l^{-1}) and
338 DIC concentrations ($\bar{x}$ = 65.4 ± 2.7 mg l^{-1}) as well as dissolved CO_2 ($\bar{x}$ = 22.3 ± 1.4 mg l^{-1}) and CH_4
339 concentrations exhibited a weak negative linear correlation (r = -0.24, p = 0.50) and a moderate positive linear
340 correlation (r = 0.42, p = 0.23), respectively.

341 $\delta^{13}C_{VPDB}$-CH_4 values ($\bar{x}$ = −57.9 ± 5.9 ‰) showed in general small variations, except for two noticeable
342 more negative values of -67.5 ‰ and -70.3 ‰ at 5 m and 12.5 m depth, respectively. Similarly, $\delta^{2}H_{SMOW}$-CH_4
343 ($\bar{x}$ = −182 ± 7 ‰) varied only little between 2.5 m to 17.5 m depth and in the further lower depths reached a
344 minimum of -218.6 ‰ at 20 m and a maximum of −188.6 ‰ at 25 m. However, $\delta^{13}C_{VPDB}$-CH_4 and $\delta^{2}H_{SMOW}$-
345 CH_4 values showed a weak positive linear correlation (r = 0.34, p < 0.001). For $\delta^{13}C_{VPDB}$-CO_2 values ($\bar{x}$ =
346 −15.4 ± 0.9 ‰) a noticeable positive value was observed in a depth of 2.5 m while in the lower part of the
347 aquifer values showed only small variations. $\delta^{13}C_{VPDB}$-CO_2 values showed a weak positive linear correlation
348 with $\delta^{13}C_{VPDB}$-CH_4 (r = 0.36, p < 0.73).

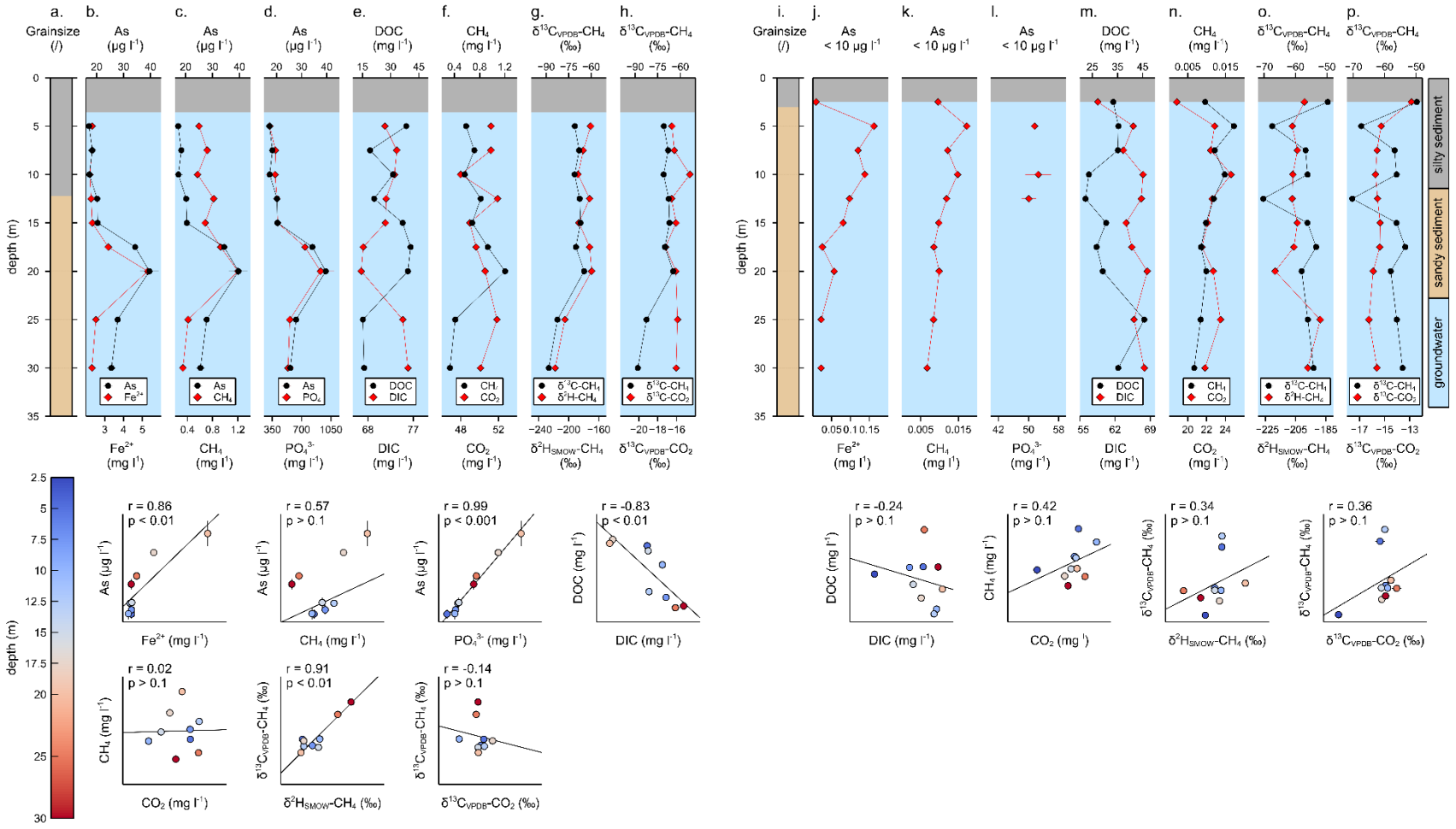

Fig 2. Depth-specific profiles of the Bera site with the respective parameters of BB1 and BB2 including grain size, the dissolved concentrations of As, Fe(II), PO_4^{3-}, DIC, DOC, CH_4, CO_2 and values of $\delta^{13}C_{VPDB}$-CH_4, $\delta^{2}H_{SMOW}$-CH_4 and $\delta^{13}C_{VPDB}$-CO_2. The colour legend for the sediment types and groundwater areas are found at the right-hand side of the depth-specific profiles. The linear relationships with coefficients of correlation (r) and *p*-values between two variables are shown below.

3.3 Korgaon site – vertical profiles of geological, geochemical and stable isotope parameters

Before water sampling, the groundwater level in KB1 was 2.93 m below ground level (Figs. 3a-h). The sediment analysis at KB1 showed grain sizes in the range of silt up to 3 m, followed by grain sizes in the range of sand up to 35 m. Dissolved As concentrations ($\bar{x}$ = 40.1 ± 13.6 µg l^{-1}) ranged from 19.1 µg l^{-1} at 2.5 m to 60.9 µg l^{-1} at 30 m and generally showed a strong with depth. Dissolved As concentrations were similar to dissolved Fe(II) ($\bar{x}$ = 63.1 ± 8.7 mg l^{-1}) and dissolved CH_4 concentrations ($\bar{x}$ = 3.6 ± 2.6 mg l^{-1}) and showed strong linear positive correlations with r of 0.87 ($p < 0.01$) and 0.82 ($p < 0.01$) for Fe(II) and CH_4, respectively. In contrast, dissolved PO_4^{3-}-concentrations ($\bar{x}$ = 1403 ± 262 µg l^{-1}) showed a decreasing pattern over depth and a strong negative linear correlation to the dissolved As concentrations (r = -0.87, $p < 0.01$). DOC ($\bar{x}$ = 35.4 ± 8.1 mg l^{-1}) and DIC concentrations ($\bar{x}$ = 71.8 ± 3.3 mg l^{-1}) showed great variability over depth and in comparison, a moderate negative linear correlation with r of -0.59 ($p < 0.01$). Dissolved CO_2 concentrations ($\bar{x}$ = 106 ± 5 mg l^{-1}) showed a maximum of 115 mg l^{-1} at 15 m depth and in the lower part of the aquifer smaller concentrations. Dissolved CO_2 concentrations to dissolved CH_4 concentrations showed a moderate negative linear correlation with a r of −0.70 ($p < 0.05$).

The $\delta^{13}C_{VPDB}$-CH_4 values ranged from −51.2 ‰ at 17.5 m to −61.3 ‰ at 30 m ($\bar{x}$ = −55.5 ± 3.9 ‰) and the $\delta^{2}H_{SMOW}$-CH_4 values from −140 ‰ at 10 m to 184 ‰ at 30 m ($\bar{x}$ = −159 ± 14 ‰) showing a great variability but in general a trend towards more negative values over depth and a weak positive linear correlation (r = 0.35, p = 0.36). Contrary to $\delta^{13}C_{VPDB}$-CH_4 values, $\delta^{13}C_{VPDB}$-CO_2 values ($\bar{x}$ = −18.9 ± 0.9 ‰) showed only a small variability with depth with a moderate negative linear correlation (r = 0.44, p = 0.24).

The groundwater level in KB2 was 1.56 m below ground level before water sampling (Figs. 3i-p). The sediment analysis at KB2 showed grain sizes in the range of silt up to 3 m and in the following grain sizes in the range of sand up to 35 m. Dissolved As concentrations could only be determined at five depths ($\bar{x}$ = 16.1 ± 4.0 µg l^{-1}) and ranged between 12.6 µg l^{-1} and 23.8 µg l^{-1} at 17.5 m and 10 m, respectively. In the remaining depths, dissolved As concentrations were below the detection limit of the analytical measurement system (< 10 µg l^{-1}). Dissolved Fe(II) ($\bar{x}$ = 16.8 ± 3.5 mg l^{-1}) and PO_4^{3-} concentrations ($\bar{x}$ = 1082 ± 242 µg l^{-1}) were high at the depths where dissolved As concentrations were detectable, but were lower compared to KB1. Both, dissolved Fe(II) and dissolved PO_4^{3-} concentrations showed relationships to dissolved As-concentrations with a strong positive linear correlation (r = 0.91, $p < 0.001$) and moderate positive linear correlation (r = 0.72, $p <$ 0.05), respectively. Dissolved CH_4 concentrations ($\bar{x}$ = 19.7 ± 3.8 mg l^{-1}) were several orders of magnitude

higher compared to KB1 and showed generally an increasing trend over depth. Dissolved CH_4 and As concentrations showed a weak negative linear correlation ($r = -0.17$, $p = 0.63$). DOC concentrations ($\bar{x} = 31.6 \pm 3.9$ mg l^{-1}) showed great variations and a noticeable maximum of 40 mg l^{-1} at 10 m, which corresponds to the maximum of the dissolved As concentration. Generally, DIC concentrations ($\bar{x} = 28.9 \pm 2.7$ mg l^{-1}) showed an increasing trend over depth and a weak positive linear correlation ($r = 0.21$, $p = 0.55$) with DOC concentrations. Similarly, dissolved CO_2 concentrations ($\bar{x} = 62.6 \pm 10.8$ mg l^{-1}) showed a decreasing trend over depth with a noticeable maximum of 83.7 mg l^{-1} at 5 m depth and a moderate negative linear correlation ($r = -0.64$, $p = 0.05$) with dissolved CH_4 concentrations.

Both, the $\delta^{13}C_{VPDB}$-CH_4 ($\bar{x} = -69.3 \pm 4.3$ ‰) ranging from −63.4 ‰ at 20 m and −75.7 ‰ at 7.5 m and the $\delta^{2}H_{SMOW}$-CH_4 values ($\bar{x} = -207 \pm 3$ ‰) ranging from −200.9 ‰ at 5 m and −211.8 ‰ at 20 m, showed a small variability and a weak negative linear correlation ($r = -0.25$, $p = 0.49$). In the depths where dissolved As was detectable, $\delta^{13}C_{VPDB}$-CH_4 and $\delta^{2}H_{SMOW}$-CH_4 values show no noticeable relationship to dissolved As concentrations. $\delta^{13}C_{VPDB}$-CO_2 values ($\bar{x} = -12.2 \pm 3.3$ ‰) showed a noticeable minimum of −20.7 ‰ at 10 m depth and a weak negative linear correlation to $\delta^{13}C_{VPDB}$-CH_4 values ($r = -0.39$, $p < 0.27$).

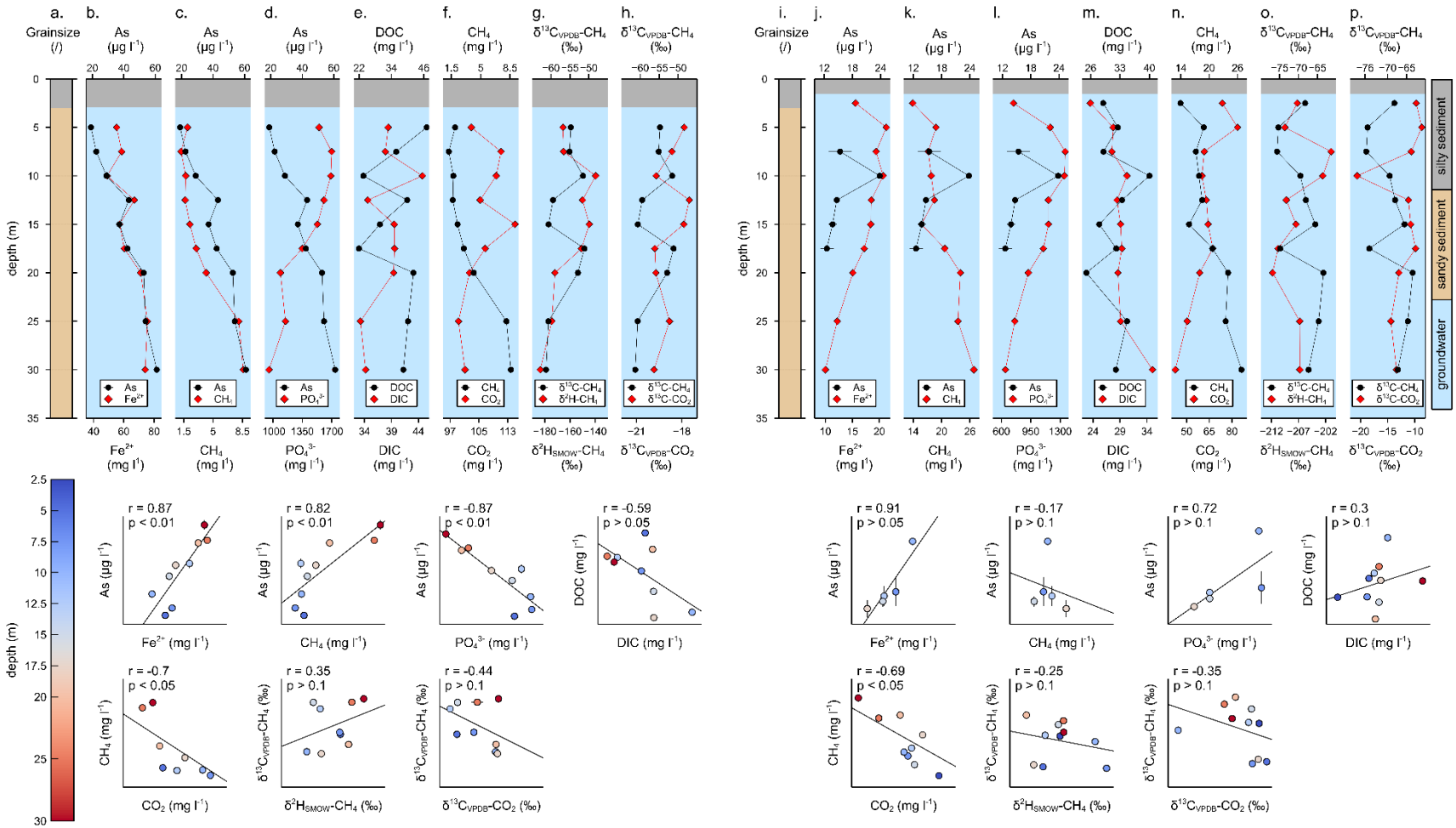

Fig 3. Depth-specific profiles of the Korgaon site with the respective parameters of KB1 and KB2 including grain size, the dissolved concentrations of As, Fe(II), PO_4^{3-}, DIC, DOC, CH_4, CO_2 and values of $\delta^{13}C_{VPDB}$-CH_4, $\delta^{2}H_{SMOW}$-CH_4 and $\delta^{13}C_{VPDB}$-CO_2. The colour legend for the sediment types and groundwater areas are found at the right-hand side of the depth-specific profiles. The linear relationships with coefficients of correlation (r) and related p-values between two variables are shown below.

3.4 Classification of CH_4 sources and pathways via stable isotope composition of CH_4, CO_2 and Bernard ratios

In order to present the results of the stable isotope data in more detail, several diagrams for the classification of CH_4 sources according to Whiticar et al. (2020) (Fig. 4) were produced in addition to the depth-specific profiles (Figs. 2 & 3). Moreover, Bernard ratios (molar ratio of $(C_1/(C_2+C_3))$ were added as another variable for better characterising the origin and fate of CH_4 in the investigated wells.

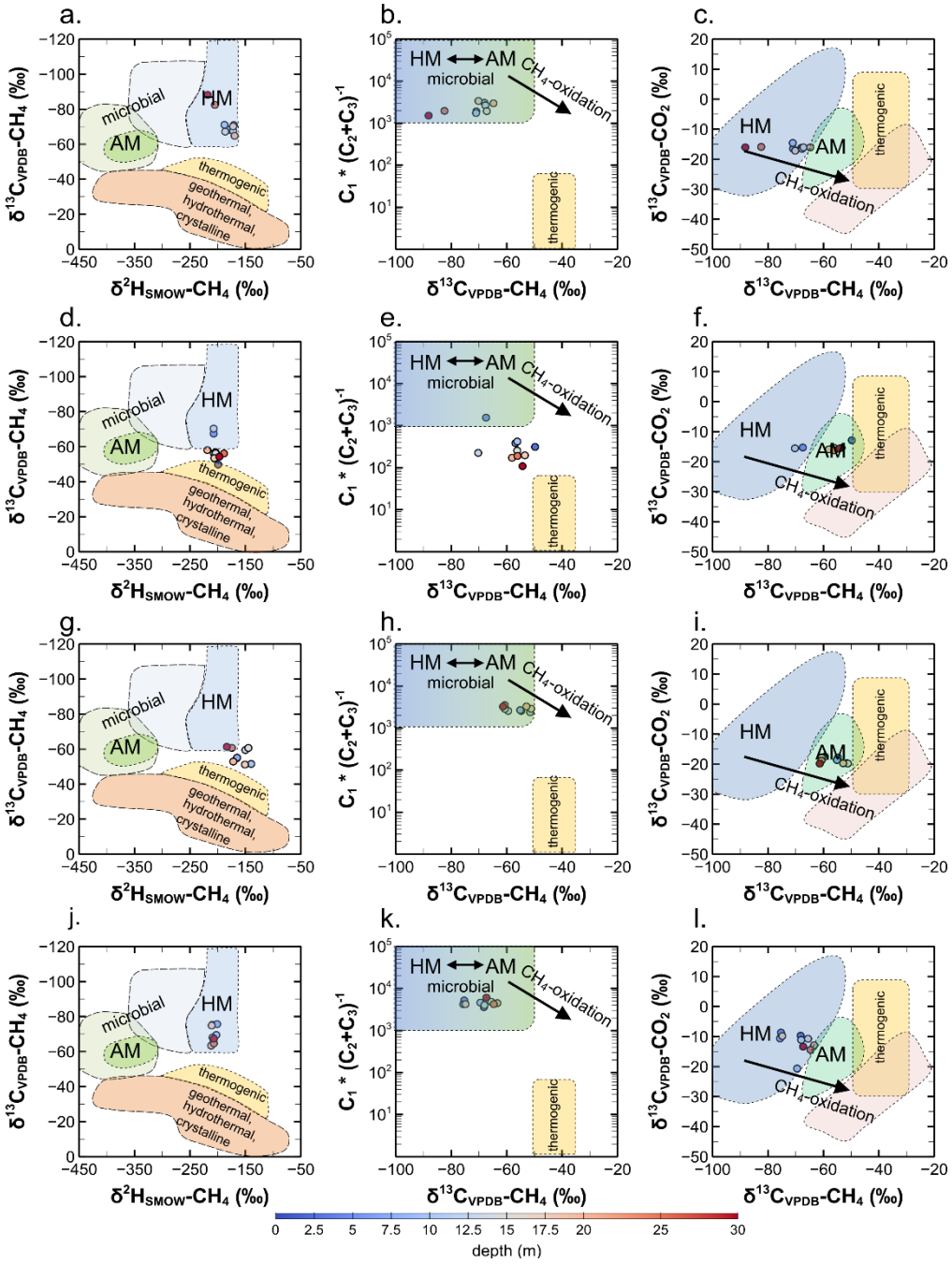

Fig 4. Classification schemes indicating the origin and fate of produced CH_4 (coloured boxes) in the investigated wells (modified after Whiticar, 2020). $\delta^{13}C_{VPDB}$-CH_4 vs $\delta^{2}H_{SMOW}$-CH_4 values (a, d, g, j), Bernard ratios $(C_1/(C_2+C_3))$ vs. $\delta^{13}C_{VPDB}$-CH_4 values (b, e, h, k) and $\delta^{13}C_{VPDB}$-CH_4 vs. $\delta^{13}C_{VPDB}$-CO_2 values (c, f, i, l)

410 are illustrated for the depth-specific profiles of BB1, BB2, KB1 and KB2, respectively. The black arrows
411 indicate the trajectory of these parameters due to aerobic CH_4 oxidation. AM and HM indicate acetoclastic and
412 hydrogenotrophic methanogenesis, respectively.

413 While in BB1 the Bernard ratios ($\bar{x}$ = 2347 ± 633) ranged between 1515 at 30 m and 3380 at 17.5 m
414 depth, the Bernard ratios in BB2 were comparatively lower ($\bar{x}$ = 381 ± 400) ranging between 108 at 30 m and
415 1549 at 5 m. At the Korgaon site, the Bernard ratios were higher than at the Bera site, with KB1 ($\bar{x}$ = 4329 ±
416 363) ranging from 2384 at 10 m to 3522 at 25 m depth and KB2 ($\bar{x}$ = 4555 ± 658) from 2597 at 2.5 m to 6082
417 at 30 m.

418 **5 Discussion**

419 First, the results from each of the four investigated wells are discussed individually, focusing on As
420 mobilisation in relation to potential CH_4 pathways. This assessment is based on measured in-situ parameters
421 and depth-specific geochemical profiles, including dissolved CH_4 and CO_2 concentrations (Figs. 2 & 3).
422 Particular focus is placed on the classification schemes of CH_4 sources and pathways in the groundwater that
423 are derived from the depth-specific profiles of stable isotopes of CH_4 and CO_2 as well as the Bernard ratios
424 (Fig. 4). These classifications are then integrated with the geochemical profiles to evaluate the interactions
425 among As, CH_4 and Fe(II). In the final part of the discussion, the four sites are compared with respect to their
426 environmental conditions and the resulting influence on CH_4 dynamics and As mobilisation.

427 **5.1 As-mobilisation and CH_4 pathways at the Bera site**

428 The well BB1 (located in the village) showed relatively high concentrations of dissolved As in the
429 groundwater throughout the whole depth profile (Fig. 2b) clearly exceeding the WHO provisional guide value
430 for drinking water of 10 µg l^{-1} in all sampled depths. However, the dissolved As concentrations exhibited a
431 noticeable variation, including comparatively low dissolved As concentrations in the upper silt layer, followed
432 by an increase with a change in the grain size to more sandy sediments, indicating that As is more mobile in
433 the lower coarser aquifer material. Although the grain size itself can influence the dissolved As concentration
434 through variable As-adsorption capacities (Maier, 2014) and different groundwater velocities (Feng et al.,
435 2022), these results indicate, that As is mobilised in the sandy sediments due to geochemical processes.

436 Considering the in-situ parameters and despite the lack missing data for dissolved O_2 concentrations,
437 the groundwater conditions can be assumed to be anoxic, as consistently low E_H values and high ECs were
438 measured, pointing to reducing conditions and high dissolved total ion concentrations. In addition, the high

dissolved Fe(II) concentration also suggests anoxic conditions and a reducing environment in which most dissolved O_2 was already consumed and Fe(III) compounds were used as electron donors instead.

As-mobilisation within the sandy sediments seemed to be driven by a redox process, as lowest E_H values correlated with the highest dissolved As concentrations. Moreover, the results of the depth-specific geochemical parameters indicate that Fe(III) (hydr)oxide reduction was responsible for the As-mobilisation. First, the strong positive linear relationship with almost identical profile patterns of the dissolved As and Fe(II) concentrations (Fig. 2b) indicated a common mobilisation process, indicative for Fe(III) (hydr)oxide reduction. In addition, the positive correlation between As and PO_4^{3-} (Fig. 2d) might be explained by Fe(III) (hydr)oxide reduction, as the profiles of As and PO_4^{3-} indicated the same mobilisation patterns. Therefore, we suggest that the competitive ion exchange between As and PO_4^{3-} might has played only a minor role for As-mobilisation in this well. Finally, similar trend in the depth-specific profiles of dissolved CH_4 and As concentrations (Fig. 2c) indicated a relationship between the two parameters regarding As mobilisation.

The profile of the dissolved CH_4 concentrations suggests that CH_4 either originated from below 20 m depth of the aquifer or was transported laterally by the groundwater flow. However, using only the observed CH_4 concentration is often an insufficient indicator to characterize the area of CH_4 formation (Hansen et al., 2001). Moreover, the measured E_H values were at least < 111 mV at all sampled depths and therefore indicated a redox environment that was not reducing enough to drive anaerobic methanogenic processes. Therefore, it is more likely that CH_4 was formed in deeper aquifer (below our deepest sampling depth) and migrated upwards in the groundwater as a result of its volatile character. CH_4 migration in groundwater has been widely discussed, especially when investigating leaks from natural gas pipelines and distinguishing them from natural formation processes (Humez et al., 2016). Various studies have shown that CH_4 migrates upwards after its formation in the groundwater and that it can then be stored and enriched depending on the permeability of the aquifer material (Cahill et al., 2017; Steelman et al., 2017). Thus, at BB1 CH_4 formation most likely took place in groundwater levels > 30 m, where methanogenic processes were driven at presumably lower E_H values and subsequently, migrated and was accumulated under the silty sediments in the area of grain size change. Although the transition from silty to sandy sediments appears at a depth of 12 m in the profiles, this boundary is not sharply defined. Moreover, due to the drilling method used, some uncertainty remains regarding the exact depth of sediment transitions. Nevertheless, based on the CH_4 concentration profile, we infer that the accumulation of dissolved CH_4 around 20 m depth is associated with changes in grain size, which likely acted

as a migration barrier. The comparatively low dissolved CH_4 concentrations in the silty sediments indicated that only little CH_4 migrated through the finer grain sizes acting as barrier due to its lower permeability. Therefore, in the depths of the highest dissolved As concentration, there was sufficient CH_4 available due to migration and accumulation of CH_4, that presumably induced Fe(III) (hydr)oxide reduction due to CH_4 oxidation, indicated by positive correlations of dissolved As, Fe(II), and CH_4 concentrations (Figs. 2b, c).

In addition, profiles of $\delta^{13}C_{VPDB}$-CH_4 and $\delta^{2}H_{SMOW}$-CH_4 values support methanogenic origin of CH_4 in the groundwater at lower depths (Fig. 2g). The observed trend towards more positive $\delta^{13}C_{VPDB}$-CH_4 and $\delta^{2}H_{SMOW}$-CH_4 values with shallower depths, suggests the occurrence of CH_4 oxidation in the groundwater due to its characteristic feature of a kinetic isotope fractionation, leading to an enrichment in ^{13}C and ^{2}H (Barker & Fritz, 1981). Especially in the depth range of 25 m to 20 m, $\delta^{13}C_{VPDB}$-CH_4 and $\delta^{2}H_{SMOW}$-CH_4 values become noticeable more positive by up to 18 ‰ and 36 ‰, respectively (Fig. 2g). Both the shift of stable isotope values towards more positive $\delta^{13}C_{VPDB}$-CH_4 and $\delta^{2}H_{SMOW}$-CH_4 values and the concurrent maximum concentrations of dissolved As, Fe(II) and CH_4 also occurring at 20 m depth, clearly indicate that As-mobilisation was related to Fe(III) (hydr)oxide reduction using CH_4 as electron donor in the groundwater. In contrast, the dissolved CO_2 concentrations as well as the $\delta^{13}C_{VPDB}$-CO_2 values in the groundwater were not indicative for the CH_4 oxidation (Fig. 2h). However, CO_2 is the end-product of many microbial processes within the groundwater and is not exclusively formed as a reaction product of CH_4 oxidation, which is why dissolved CO_2-concentrations and $\delta^{13}C_{VPDB}$-CO_2 values were likely affected by many different processes and were therefore highly variable (Stopelli et al., 2021, Whiticar et al., 2020).

The origin and the further reaction pathways of CH_4 were also inferred by using stable isotope data in combination with Bernard ratios (Figs. 4a, b, c). Using the classification schemes of Whiticar et al. (2020) the combination of $\delta^{13}C_{VPDB}$-CH_4 and $\delta^{2}H_{SMOW}$-CH_4 values clearly indicated biogenic CH_4 at all sampled depths, more precisely hydrogenotrophic methanogenesis (Fig. 4a). However, Bernard ratios with $\delta^{13}C_{VPDB}$-CH_4 values pointed more towards a mixed origin of hydrogenotrophic and acetoclastic methanogenesis (Fig. 4b). Nevertheless, it is more likely that CH_4 was formed by hydrogenotrophic methanogenesis and the more positive $\delta^{13}C_{VPDB}$-CH_4 values that assign CH_4 to an acetoclastic origin in this diagram were solely the result of CH_4 oxidation in the groundwater. Furthermore, the distribution of the data points in Fig. 4b were not characteristic of the typical course of CH_4 oxidation, due to the low Bernard ratios at 25 m and 30 m depth. Although the Bernard ratios at these depths result in data point distributions do not correspond to CH_4

497 oxidation, they still support the proposed CH_4 migration from higher depths, as the highest Bernard ratios were
498 measured in the areas of highest dissolved CH_4 concentrations. Moreover, the combination of $\delta^{13}C_{VPDB}$-CH_4
499 and $\delta^{13}C_{VPDB}$-CO_2 values (Fig. 4c) showed that the distribution of the data points corresponded to the typical
500 trend of CH_4 oxidation and thus takes place in the groundwater, although the low Bernard ratios at 25 m and
501 30 m depth differed as a result of CH_4 migration.

502 The well BB2 (agricultural site) showed dissolved As concentrations < 10 µg l^{-1} at all sampled depths
503 in the groundwater (Fig. 2j) indicating that As-mobilisation in this aquifer is limited. There was no change in
504 grain size in the aquifer material considered and only sandy sediments were present, which is why the influence
505 of grain size on the As concentration through As-adsorption capacity can be ruled out and it is more likely that
506 the prevalent geochemical conditions lead to the absence of dissolved As.

507 Based on the measured in-situ parameters the aquifer might be slightly reducing, as consistently high
508 E_H values and low conductivities and low dissolved total ion concentration were measured. Thus, the redox
509 milieu was probably not sufficiently reducing to affect redox-processes like Fe(III) mineral reduction, that
510 could subsequently contribute to As-mobilisation in the groundwater. In addition, low dissolved Fe(II)
511 concentrations point to rather hypoxic than anoxic conditions, in which Fe(III) (hydr)oxides are stable.
512 Moreover, considering that dissolved PO_4^{3-} was mostly not detectable or only found at very low concentrations
513 (Fig. 2l), the aquifer at BB2 might contain As and PO_4^{3-} mainly adsorbed at the surfaces of Fe(III) (hydr)oxides.
514 Finally, the depth-specific profile of the dissolved CH_4 concentrations did not indicate a clear CH_4 source (Fig.
515 2k). The high E_H-values prevent conditions that favors microbial CH_4 formation.

516 Besides the geochemical profiles, also the stable isotope profiles did not infer concrete CH_4 sources
517 and sinks in the groundwater. $\delta^{13}C_{VPDB}$-CH_4 and $\delta^{2}H_{SMOW}$-CH_4 values showed a weak positive linear correlation
518 and different depth-specific profiles (Fig. 2o), which is not characteristic for CH_4 oxidation, since the kinetic
519 isotope fractionation should result in a shift towards more positive δ-values for both $\delta^{13}C_{VPDB}$-CH_4 and
520 $\delta^{2}H_{SMOW}$-CH_4 values. Moreover, depth-specific $\delta^{13}C_{VPDB}$-CO_2 values exhibited only small variations in the
521 groundwater, thus also showed no clear characteristic trends for CH_4 oxidation (Fig. 2p).

522 The stable isotope data in combination with measured Bernard ratios provide additional information
523 on the potential formation and degradation pathways of CH_4 (Figs. 4d, e, f). The combination of $\delta^{13}C_{VPDB}$-CH_4
524 values and $\delta^{2}H_{SMOW}$-CH_4 values indicated different origins of CH_4 (Fig. 4d). While CH_4 at 12.5 m and 5 m
525 were characterised by hydrogenotrophic methanogenesis, the CH_4 in the remaining depths were located in the

transition zone or in the area characteristic for CH_4, formed due thermogenic processes. However, BB2 is not located near any known natural gas deposits (Shetol et al., 2019), therefore the occurrence of thermogenic CH_4 is unlikely and CH_4 is presumably formed biogenic by methanogenic processes. Moreover, the combination of $\delta^{13}C_{VPDB}$-CH_4 values and Bernard ratios points to a biogenic CH_4 formation in all sampled depths, however not exclusively by hydrogenotrophic methanogenesis, but also by acetoclastic methanogenesis (Fig. 4e). Although, it is not entirely clear whether CH_4 was formed from hydrogenotrophic or acetoclastic formation pathways, the results imply clearly that CH_4 was formed biogenic due methanogenesis. Furthermore, the distribution of the data points does not correspond to the characteristic course of CH_4 oxidation since shifts in $\delta^{13}C_{VPDB}$-CH_4 values and Bernard ratios are not indicative. Finally, the combination of $\delta^{13}C_{VPDB}$-CH_4 and $\delta^{13}C_{VPDB}$-CO_2 values show no indicative pathways, which is due to the small variations of $\delta^{13}C_{VPDB}$-CO_2 values in the groundwater, resulting in a point distribution corresponding to a horizontal line not characteristic for CH_4 oxidation (Fig. 4f). Based on the constrains off all measured parameters it seemed that CH_4 did not have a substantial influence on As-mobilising redox processes at the agricultural site BB2.

5.2 As-Mobilisation and CH_4 pathways at the Korgaon site

The well KB1 (village site) showed high dissolved As concentrations (up to 61 µg l^{-1}) in the groundwater throughout the whole depth-specific profile (Fig. 3b) drastically exceeding the WHO recommended limit of 10 µg l^{-1} in all sampled depths. The pattern of the dissolved As concentrations in the depth-specific profile indicated an increased As-mobilisation with increasing depth. Because there was no change in grain size in the aquifer material considered and only sandy sediments were present, the influence of grain size on the As concentration through As-adsorption was unlikely and it is highly likely that the prevalent geochemical conditions controlled to As-mobilisation.

Based on the measured in-situ parameters the aquifer at KB1 can be assumed to be predominantly anoxic, as consistently the low E_H values as well as high ECs were measured, pointing to reducing conditions and high dissolved total ion concentration. Moreover, the high dissolved Fe(II) concentration indicate anoxic conditions and a reducing environment in which dissolved O_2 was already consumed and Fe(III) compounds were used as electron donors instead.

As-mobilisation seems to be driven by a redox process, since E_H values are low and correlate with the dissolved As concentrations. In addition, the depth-specific profile of dissolved Fe(II) concentrations shows an almost identical course with a high correlation to the profiles of the dissolved As-concentrations and

555 dissolved CH_4 concentrations (Figs. 3b, c), indicating strong relationship between As, Fe(II) and CH_4, most
556 likely by CH_4 oxidation. However, although the E_H values are relatively low, they are too high for a redox
557 environment supporting methanogenic processes, which is why it is more likely that CH_4 is formed in deeper
558 aquifer areas > 30 m where E_H values are presumably lower and subsequent, CH_4 migrates in the groundwater.
559 However, it is somewhat unusual that CH_4 is not trapped below the silty sediments on the top acting as natural
560 CH_4 barrier, as often observed in other wells. This is presumably caused by degradation due to pronounced
561 CH_4 oxidation, which consumes the upward migrating CH_4 and therefore not much CH_4 is accumulated under
562 of the silty sediments, In addition, the negative correlation and depth-specific profiles supports the distinct
563 CH_4 oxidation in the groundwater. However, the negative correlation of dissolved As and PO_4^{3-} concentrations
564 (Fig. 3d) indicate that simultaneously to CH_4 oxidation, competitive ion exchange processes between As and
565 PO_4^{3-} on mineral surfaces contribute to As-mobilisation at KB1, as a positive correlation would be expected if
566 both, As and PO_4^{3-} are mobilised by the same process in the groundwater.

567 In addition to geochemical data, the depth-specific profiles of stable isotope ratios are indicative favour
568 for active CH_4 pathways in the groundwater. Although $\delta^{13}C_{VPDB}$-CH_4 and $\delta^{2}H_{SMOW}$-CH_4 values show a weak
569 positive linear correlation, they exhibit a similar depth-specific pattern including progressively more positive
570 values with shallower depth (Fig. 3g), which is a characteristic feature of a kinetic isotope fractionation due to
571 CH_4 oxidation. Moreover, the depth-specific $\delta^{13}C_{VPDB}$-CO_2 values show a moderate negative linear correlation
572 to $\delta^{13}C_{VPDB}$-CH_4 values in the groundwater (Fig. 3h), clearly indicating that a fraction of CO_2 carbon is derived
573 from CH_4 oxidation in the groundwater.

574 The classification schemes of Whiticar et al. (2020) also inferred the origin and the further reaction
575 pathways of CH_4 (Figs. 4g, h, i). The combination of $\delta^{13}C_{VPDB}$-CH_4 values and $\delta^{2}H_{SMOW}$-CH_4 values indicate
576 that CH_4 in all sampled depths was mainly characterised between biotic and thermogenic formation fields (Fig.
577 4g). Although natural gas deposits exist around the Korgaon site (Shetol et al., 2019), the combination of
578 Bernard ratios with the $\delta^{13}C_{VPDB}$-CH_4 values suggests clearly a biogenic CH_4 formation, presumably
579 acetoclastic methanogenesis (Fig. 4h). Moreover, the distribution of the data points in this diagram is
580 characteristic of the typical course of CH_4 oxidation, which is due to the lower Bernard ratios and more positive
581 $\delta^{13}C_{VPDB}$-CH_4 values with decreasing depth. Thus, the position of the data points between the biotic and
582 thermogenic formation fields is most probably a result of occurring CH_4 oxidation and associated kinetic
583 isotope fractionation of $\delta^{13}C_{VPDB}$-CH_4 (Barker & Fritz, 1981). Moreover, the combination of $\delta^{13}C_{VPDB}$-CH_4 and

584 $\delta^{13}C_{VPDB}$-CO_2 values further points to that the distribution of the data points corresponding to the typical trend
585 of CH_4 oxidation (Fig. 4i).

586 The well KB2 (agricultural site) shows only in five sampled depths detectable dissolved As
587 concentrations, which are lower than 24 µg l^{-1} (Fig. 3j) and thus only slightly exceeded the recommendation
588 of the WHO. Because there is no change in grain size in the aquifer material considered and only sandy
589 sediments are present, the influence of grain size on the dissolved As concentration through As-adsorption
590 capacity is unlikely. Therefore, it can be assumed, that the prevalent geochemical conditions lead to the high
591 dissolved As concentrations in five depths. However, please note that in this well the correlations of depth-
592 specific profiles to dissolved As concentrations are based on limited data of only five data points.

593 The depth-specific profile of dissolved Fe(II) concentrations shows a similar course with a high
594 correlation to the profiles of the dissolved As concentrations (Fig. 3j), indicating a common mobilisation
595 process for As and Fe(II). Moreover, depth-specific PO_4^{3-} concentrations correlate with dissolved
596 concentrations of As and Fe(II) (Fig. 3l), which is likely due both, As and PO_4^{3-}, are mobilised by Fe(III)
597 (hydr)oxide-reduction. Although CH_4 concentrations in groundwater are high, the depth-specific profile shows
598 no correlation between CH_4 with As or $Fe^{(II)}$ (Fig. 3k), making it unlikely that CH_4 was related to As-
599 mobilisation. Again, E_H values are too high for a redox environment supporting methanogenic processes in the
600 depth of the investigated well, and thus it is more likely that CH_4 is formed in deeper aquifer areas > 30 m
601 where E_H values are presumably lower and subsequent CH_4 migrates in the groundwater upwards. In addition,
602 the depth-specific profile of CH_4 indicates, that CH_4 oxidation strongly occurred in the groundwater, since CH_4
603 concentrations decrease upwards, indicating consumption of the upward migrating CH_4 and no CH_4 is
604 accumulating under the silty sediments.

605 Although CH_4 concentrations in the groundwater points indicate CH_4 degradation, the depth-specific
606 profiles of stable isotope ratios do not confirm active CH_4 oxidation pathways in the groundwater. The depth-
607 specific profiles of $\delta^{13}C_{VPDB}$-CH_4 and $\delta^{2}H_{SMOW}$-CH_4 values show a weak negative linear correlation and neither
608 $\delta^{13}C_{VPDB}$-CH_4 nor $\delta^{2}H_{SMOW}$-CH_4 presenting clear trends (Fig. 3o). However, the profile of $\delta^{13}C_{VPDB}$-CO_2 values
609 showed a distinct minimum at 10 m depth, concurring with a maximum of dissolved As and DOC
610 concentrations (Figs. 3j, m). This could be an indicator for As-mobilisation as a result of a CO_2-forming redox
611 reaction using highly available dissolved organic compounds at 10 m depth. The stable isotope data in
612 combination with measured Bernard ratios provide further insights into the potential origin and fate of CH_4

(Figs. 4j, k, l). The combination of $\delta^{13}C_{VPDB}$-CH_4 values and $\delta^{2}H_{SMOW}$-CH_4 values indicate that CH_4 in all sampled depths was mainly characterised by hydrogenotrophic methanogenesis (Fig. 4j). However, the combination of Bernard ratios with the $\delta^{13}C_{VPDB}$-CH_4 values suggests a biogenic CH_4 formation by acetoclastic methanogenesis (Fig. 4k). Therefore, based on the three CH_4 characterisation plots the formation pathway of biogenic CH_4 at KB2 is not clear. However, a mixture of both hydrogenotrophic and acetoclastic methanogenesis is the most probable scenario. Furthermore, the distribution of the data points in Fig. 4k corresponds to a horizontal line and is not characteristic of the typical course of CH_4 oxidation, due to the Bernard ratios, that are almost constant in the depth-specific profile. Finally, the combination of $\delta^{13}C_{VPDB}$-CH_4 and $\delta^{13}C_{VPDB}$-CO_2 values also shows that the distribution of the data points does not correspond to the typical trend of CH_4 oxidation (Fig. 4l) and thus it is unlikely that CH_4 oxidation is strongly involved in As-mobilisation at this site.

5.3 Comparison of all four wells

Considering the results from the four wells the following pattern might be suggested: The two wells in the villages BB1 and KB1 generally contain substantially more dissolved As compared to the two wells on agricultural areas BB2 and KB2. Moreover, the two wells in the villages show higher dissolved Fe(II) concentrations and lower E_H-values compared to the respective well on the agricultural area. The redox conditions in the two wells within the villages were generally more reducing, potentially leading to the dissolution of Fe(III) (hydr)oxides and subsequently mobilisation of As. Surprisingly the DOC concentrations of all four wells were in a similar range (Figs. 2e, m & Figs. 3e, m), indicating a high availability of electron donors affecting reducing conditions in all wells. However, measured DOC concentrations represents a sum parameter of organic matter and does not provide further insight into specific organic molecules. A possible explanation for this observation has been described in several studies, presenting different composition and bioavailability of the initial organic carbon as a key parameter affecting As-contaminations between village and agricultural environments (Anawar et al., 2023; Neumann et al., 2010, 2014). Organic carbon in village environments mainly originates from wastewater of latrines, consisting of labile, low-molecular organic carbon compounds, which are easily microbially degradable and therefore drive redox processes as electron donors including as Fe(III) (hydro)oxide reduction and subsequent As-mobilisation (Anawar et al., 2013; Berggren et al., 2010). In contrast, organic carbon in agricultural environments usually consists of more complex plant-based molecules, with lower bioavailability and higher resistance to microbiological degradation which rather

limits its role as an electron donor (Neumann et al., 2010). However, the dissolved organic carbon of the four wells was not further analysed for its specific molecular composition, age or source, and thus no further conclusion about the bioavailability of the organic matter in the four wells might be drawn.

Based on the depth-specific patterns of CH_4 concentrations and their stable isotope values as well as the associated Bernard ratios, a potential important role of CH_4 cycling in As release in the village sites BB1 and KB1 has been revealed. Moreover, the results of the wells BB2 and KB2 on the agricultural areas did not show an obvious influence of CH_4 on As-mobilisation due to CH_4 oxidation. The results show more variable CH_4 occurrences between BB2 and KB2, which have to be differentiated in future research. Although the well KB2 is located on an agricultural area, has higher E_H values and lower concentrations of As and Fe(II) compared to KB1, it also shows the highest dissolved CH_4 concentrations of all the wells examined. Most likely CH_4 was formed due to methanogenic processes by the degradation of sedimentary organic carbon (SOC), which is available in deeper sections of the aquifer. Such old SOC deposits form a potentially bioavailable organic carbon source in the sand layers (Mailoux et al., 2013; Neumann et al., 2014), which may provide deep methanogenic conditions at KB2 and thus, influence the As-mobilisation. Moreover, the sediment analysis at KB2 at a depth of 42.7 m (App. 2) showed a black coloured layer that is rich in organic material, which serves as a potential source of bioavailable organic carbon in the groundwater and drives formation and migration of CH_4. Although there were high concentrations of CH_4 found in KB2, As concentrations were only detectable at 5 depths, making a strong relationship between CH_4 and As-mobilisation at this location unlikely. However, the result of low dissolved As concentrations only detectable at five depths and sufficiently available CH_4 can also be explained by a limitation of sedimentary As deposits on Fe(III) (hydr)oxides to the depths from 7.5 m to 17.5 m, and therefore As mobilisation is restricted to this section of the aquifer.

6 Conclusion

In this study, we investigated four groundwater wells in northern Bangladesh using depth-specific sampling and a comprehensive set of hydrobiogeochemical measurements, with a particular focus on the role of CH_4 cycling in arsenic mobilisation. Two of the wells significantly exceeded the WHO provisional guideline value for dissolved As, while the other two displayed lower concentrations. Importantly, As levels not only varied between wells but also showed distinct depth-specific profiles, highlighting the site-specific nature and complexity of As mobilisation processes in these aquifers.

A central aim of this study was to explore the link between CH_4 oxidation, Fe(III) reduction, and As release under natural field conditions, a relationship that has so far been predominantly studied in laboratory incubations. Using depth-resolved isotope measurements of CH_4 and CO_2, alongside Bernard ratios, we were able to identify the sources and transformation pathways of CH_4 in the subsurface. The isotopic data revealed clear evidence for methanogenic CH_4 formation in deeper aquifer zones (>30 m), followed by upward migration and partial oxidation near zones of sedimentary transition. Isotopic enrichment patterns strongly suggest CH_4 oxidation, most likely coupled to Fe(III) (hydr)oxide reduction. This CH_4-driven mechanism of Fe reduction and subsequent As mobilization was particularly evident in two of the wells located in village settings. In these wells, positive correlations between dissolved CH_4, Fe(II), and As concentrations were consistent with zones of CH_4 oxidation inferred from isotopic shifts. In contrast, a well located at an agricultural site showed the highest CH_4 concentrations but relatively low As levels, with isotope data indicating limited CH_4 oxidation, suggesting that the presence of CH_4 alone is not sufficient to trigger As release. These results provide the first field-based isotopic evidence supporting a pathway of CH_4-fueled Fe(III) reduction and associated As mobilization in Bangladeshi aquifers. They also highlight that this process is highly site-specific, governed by local hydro-biogeochemical conditions such as redox gradients, sediment structure, and microbial activity. Our findings underscore the importance of integrating isotopic, geochemical, and microbiological approaches to disentangle the complex interplay between CH_4 cycling and As mobilization. We recommend further interdisciplinary field studies that combine inorganic and organic geochemistry, stable isotope techniques, and microbial analyses to deepen our understanding of CH_4–Fe–As interactions in As-affected aquifers.

Credit authorship contribution statement

Kai Ernst: Methodology, Formal analysis, Investigation, Writing – Original Draft, Writing – Review & Editing, Visualization. **Charlotte Stirn:** Formal analysis, Investigation, Writing – Review & Editing Project administration, Funding acquisition. **Martin Maier:** Formal analysis, Investigation, Writing – Review & Editing, Project administration, Funding acquisition. **Moritz Schroll:** Methodology, Formal analysis, Writing – Review & Editing. **David Polya:** Conceptualization, Methodology, Writing – Review & Editing. **Frank Keppler:** Conceptualization, Methodology, Resources, Writing – Review & Editing, Supervision, Project administration, Funding acquisition.

Data availability

Data will be made available upon request.

Acknowledgements

Funding was provided by the Heidelberg Center for the Environment (HCE) through the excellence strategy and the Forschungspool of Heidelberg University. We thank Marcus Schneider, Markus Greule, Bernd Knape, Christian Scholz, Silvia & Stefan Rheinberger for technical and analytical support.

Declaration of generative AI and AI-assisted technologies in the writing process

During the preparation of this work the author(s) used ChatGPT version 4.0 in order to rephrase text. After using this tool/service, the author(s) reviewed and edited the content as needed and take(s) full responsibility for the content of the publication.

References

Akoglu H. (2018). User's guide to correlation coefficients. *Turk J Emerg Med*, 18(3), 91-93. https://doi.org/10.1016/j.tjem.2018.08.001.

Anawar, H. M., Tareq, S. M., Ahmed, G. (2013). Is organic matter a source or redox driver or both for arsenic release in groundwater?. *Phys. Chem. Earth.*, 58–60, 49–56. https://doi.org/10.1016/j.pce.2013.04.009.

728 Appelo, C. A. J., Postma, D. (2005). Geochemistry, groundwater and pollution. 2nd edition, CRC Press, Taylor
729 & Francis Group, Boca Raton, London, New York. https://doi.org/10.1201/9781439833544.

730 Barker, J. F., Fritz, P. (1981). Carbon isotope fractionation during microbial methane oxidation. *Nature*, 293:
731 289-291. https://doi.org/10.1038/293289a0.

732 Beeman, R. E., Suflita, J. M. (1990). Environmental factors influencing methanogenesis in a shallow anoxic
733 aquifer: a field and laboratory study. *J Ind Microbiol.*, 5(1), 45-57.
734 https://doi.org/10.1007/BF01569605.

735 Berggren, M., Ström, L., Laudon, H., Karlsson, J., Jonsson, A., Giesler, R., Bergström, A.-K., Jansson, M.
736 (2010). Lake secondary production fueled by rapid transfer of low molecular weight organic carbon
737 from terrestrial sources to aquatic consumers. *Ecol. Lett.*, 13(7), 870–880.
738 https://doi.org/10.1111/j.1461-0248.2010.01483.

739 BGS and DPHE (2001). Arsenic contamination of groundwater in Bangladesh. In: Kinniburgh, D. G. and
740 Smedley, P. L. (Eds.). British geological survey report. WC/00/19. British Geological Survey,
741 Keyworth, UK. https://nora.nerc.ac.uk/id/eprint/11986.

742 Bhattacharya, P., Polya, D.A., Jovanovic. D. (Eds.) (2017). Best practice guide for the control of arsenic in
743 drinking water, IWA Publishing, London, UK. https://doi.org/10.2166/9781780404929.

744 Cahill, A. G., Steelman, C. M., Forde, O., Kuloyo, O., Emil Ruff, S., Mayer, B., Ulrich Mayer, K., Strous, M.,
745 Cathryn Ryan, M., Cherry, J. A., Parker, B. L. (2017). Mobility and persistence of methane in
746 groundwater in a controlled-release field experiment. *Nat. Geosci.*, 10(4), 289–294.
747 https://doi.org/10.1038/ngeo2919

748 Charlet L., Polya D. A. (2006). Arsenic in shallow, reducing groundwaters in southern asia: an environmental
749 health disaster. *Elements*, 2, 91-96. https://doi.org/10.2113/gselements.2.2.91.

750 Craig, H. (1957). Isotopic standards for carbon and oxygen and correction factors for mass-spectrometric
751 analysis of carbon dioxide. *Geochim. Cosmochim. Acta*, 12, 133–149. https://doi.org/10.1016/0016-
752 7037(57)90024-8.

753 Dhar, R.K., Biswas, B.K., Samanta, G., Mandal, B.K., Chakraborti, D., Roy, S., Jafar, A., Islam, A., Ara, G.,
754 Kabir, S., Khan, A.W., Ahmed, S.A., Hadi, S.A. (1997). Groundwater arsenic calamity in Bangladesh.
755 *Current Science*, 73(1), 48-59. https://www.jstor.org/stable/24098145.

756 Dumont, M. G., Murrell, J. C. (2005). Community-level analysis: Key genes of aerobic methane oxidation.
757 *Methods Enzymol.*, 397, 413–427. https://doi.org/10.1016/S0076-6879(05)97025-0.

758 Feng, S., Guo, H., Sun, X., Han, S., Li, Y. (2022). Relative importance of hydrogeochemical and
759 hydrogeological processes on arsenic enrichment in groundwater of the Yinchuan Basin, China. *Appl.*
760 *Geochem.*, 137, 105180. https://doi.org/10.1016/j.apgeochem.2021.105180.

761 Glodowska, M., Stopelli, E., Schneider, M., Lightfoot, A., Rathi, B., Straub, D., Patzner, M., Duyen, V. T.,
762 Berg, M., Kleindienst, S., Kappler, A. (2020). Role of in situ natural organic matter in mobilizing As
763 during microbial reduction of Fe(III)-mineral-bearing aquifer sediments from Hanoi (Vietnam).
764 *Environ. Sci. Technol.*, 54(7), 4149–4159. https://doi.org/10.1021/acs.est.9b07183.

765 Glodowska, M., Stopelli, E., Straub, D., Vu Thi, D., Trang, P. T. K., Viet, P. H., AdvectAs team members, Berg,
766 M., Kappler, A., Kleindienst, S. (2021). Arsenic behavior in groundwater in Hanoi (Vietnam)
767 influenced by a complex biogeochemical network of iron, methane, and sulfur cycling. *J. Hazard.*
768 *Mater.*, 407, 124398. Doi:10.1016/j.jhazmat.2020.124398.

769 Goevert, D., Conrad, R. (2009). Effect of substrate concentration on carbon isotope fractionation during
770 acetoclastic methanogenesis by *Methanosarcina barkeri* and *M. acetivorans* and in rice field soil. *Appl.*
771 *Environ. Microbiol.*, 75(9), 2605–2612. https://doi.org/10.1128/AEM.02680-08.

772 Hansen, L.K., Jakobson, R., Postma, D. (2001). Methanogenesis in a shallow sandy aquifer, Rømø, Denmark.
773 *Geochim. Cosmochim. Acta*, 65, 2925–2935. https://doi.org/10.1016/S0016-7037(01)00653-6.

774 Harvey, C. F., Swartz, C. H., Badruzzaman, A. B. M., Keon-Blute, N., Yu, W., Ashraf Ali, M., Jay, J., Beckie,
775 R., Niedan, V., Brabander, D., Oates, P. M., Ashfaque, K. N., Islam, S., Hemond, H. F., and Ahmed,
776 M. F. (2002). Arsenic mobility and groundwater extraction in Bangladesh. *Science*, 298, 1602-1606.
777 https://doi.org/10.1126/science.1076978.

778 Holler, T. (2010). Mikrobiologische Studien zur anaeroben Oxidation von Methan (AOM). Bremen University.
779 http://nbn-resolving.de/urn:nbn:de:gbv:46-00102165-17 (PhD thesis).

780 Horneman, A., van Geen, A., Kent, D. v., Mathe, P. E., Zheng, Y., Dhar, R. K., O'Connell, S., Hoque, M. A.,
781 Aziz, Z., Shamsudduha, M., Seddique, A. A., Ahmed, K. M. (2004). Decoupling of As and Fe release
782 to Bangladesh groundwater under reducing conditions. Part I: Evidence from sediment profiles.
783 *Geochim. Cosmochim. Acta*, 68(17), 3459–3473. https://doi.org/10.1016/j.gca.2004.01.026.

784 Humez, P., Mayer, B., Nightingale, M., Becker, V., Kingston, A., Taylor, S., Bayegnak, G., Millot, R.,
785 Kloppmann, W. (2016). Redox controls on methane formation, migration and fate in shallow aquifers.
786 *Hydrol. Earth Syst. Sci.*, 20(7), 2759–2777. https://doi.org/10.5194/hess-20-2759-2016.

787 Islam, F.S., Gault, A.G., Boothman, C., Polya, D.A., Charnock, J.M., Chatterjee, D., Lloyd, J. R. (2004) Role
788 of metal reducing bacteria in arsenic release in Bengal Delta sediments. *Nature*, 430, 68-71.
789 https://doi.org/10.1038/nature02638.

790 Kleikemper, J., Pombo, S., Schroth, M., Sigler, W., Pesaro, M., Zeyer, J. (2005). Activity and diversity of
791 methanogens in a petroleum hydrocarbon-contaminated aquifer. *Appl. Environ. Microbiol.*, 71, 149-
792 58. https://doi.org/10.1128/AEM.71.1.149-158.2005.

793 Knittel, K., Boetius, A. (2009). Anaerobic oxidation of methane: Progress with an unknown process. *Annu.*
794 *Rev. Microbiol.*, 63(1), 311–334. https://doi.org/10.1146/annurev.micro.61.080706.093130.

795 Liu, T. K., Chen, K. Y., Yang, T. F., Chen, Y. G., Chen, W. F., Kang, S. C., Lee, C. P. (2009). Origin of methane
796 in high-arsenic groundwater of Taiwan - Evidence from stable isotope analyses and radiocarbon dating.
797 *J. Asian Earth Sci.*, 36(4–5), 364–370. https://doi.org/10.1016/j.jseaes.2009.06.009.

798 Maier, M. (2014). Untersuchungen zum reaktiven Transport von Arsen im Grundwasserleiter, Prozessstudie
799 und Entwicklung einer neuen Sanierungsmethode an einem Altstandort in Hessen, Deutschland.
800 Heidelberg University. https://doi.org/10.11588/heidok.00017162 (PhD thesis).

801 Mailloux, B. J., Trembath-Reichert, E., Cheung, J., Watson, M., Stute, M., Freyer, G. A., Ferguson, A. S.,
802 Ahmed, K. M., Alam, M. J., Buchholz, B. A., Thomas, J., Layton, A. C., Zheng, Y., Bostick, B. C., van
803 Geen, A. (2013). Advection of surface-derived organic carbon fuels microbial reduction in Bangladesh
804 groundwater. *PNAS*, 110(14), 5331–5335. https://doi.org/10.1073/pnas.1213141110.

Mohammed Abdul, K. S., Jayasinghe, S. S., Chandana, E. P. S., Jayasumana, C., de Silva, P. M. C. S. (2015). Arsenic and human health effects: A review. *Environ. Toxicol. Pharmacol.*, 40(3), 828–846. https://doi.org/10.1016/j.etap.2015.09.016.

Moore, O. C., Xiu, W., Guo, H., Polya, D. A., van Dongen, B. E., Lloyd, J. R. (2023). The role of electron donors in arsenic-release by redox-transformation of iron oxide minerals – A review. *Chem. Geol.*, 619, 121322. https://doi.org/10.1016/j.chemgeo.2023.121322

Neumann, R. B., Ashfaque, K. N., Badruzzaman, A. B. M., Ashraf Ali, M., Shoemaker, J. K., Harvey, C. F. (2010). Anthropogenic influences on groundwater arsenic concentrations in Bangladesh. *Nat. Geosci.*, 3(1), 46–52. https://doi.org/10.1038/ngeo685.

Neumann, R. B., Pracht, L. E., Polizzotto, M. L., Badruzzaman, A. B. M., Ali, M. A. (2014). Biodegradable organic carbon in sediments of an arsenic-contaminated aquifer in Bangladesh. *Environ. Sci. Technol. Lett.*, 1(4), 221–225. https://doi.org/10.1021/ez5000644.

Paul, D., Skrzypek, G., Fórizs, I. (2007). Normalization of measured stable isotopic compositions to isotope reference scales - A review. *Rapid Commun. Mass Spectrom.*, 21(18), 3006–3014. https://doi.org/10.1002/rcm.3185.

Pienkowska, A., Glodowska, M., Mansor, M., Buchner, D., Straub, D., Kleindienst, S., Kappler, A. (2021). Isotopic labeling reveals microbial methane oxidation coupled to Fe(III) mineral reduction in sediments from an As-contaminated aquifer. *Environ. Sci. Technol. Lett.*, 8(9), 832–837. https://doi.org/10.1021/acs.estlett.1c00553.

Polya, D. A., Sparrenbom, C., Datta, S., Guo, H. (2019). Groundwater arsenic biogeochemistry – Key questions and use of tracers to understand arsenic-prone groundwater systems. *Geosci. Front.*, 10(5), 1635–1641. https://doi.org/10.1016/j.gsf.2019.05.004.

Rowland, H. A. L., Polya, D. A., Lloyd, J. R., Pancost, R. D. (2006). Characterisation of organic matter in a shallow, reducing, arsenic-rich aquifer, West Bengal. *Org. Geochem.*, 37(9), 1101–1114. https://doi.org/10.1016/j.orggeochem.2006.04.011.

Reza S., Jean, J. S. (2012). Vertical distribution and mobilization of arsenic in shallow alluvial aquifers of Chapai-Nawabganj district, Northwestern Bangladesh. *J. Geol. Soc. India*, 80, 531–538. https://doi.org/10.1007/s12594-012-0173-1.

Shetol, M., Moklesur Rahman, M., Sarder, R., Ismail Hossain, M., Kabir Riday, F. (2019). Present status of Bangladesh gas fields and future development: A review. *J. Nat. Gas Geosci.*, 4(6), 347–354. https://doi.org/10.1016/j.jnggs.2019.10.005.

Smith, A. H., Steinmaus, C. M. (2009). Health effects of arsenic and chromium in drinking water: Recent human findings. *Annu. Rev. Public Health*, 30, 107–122. https://doi.org/10.1146/annurev.publhealth.031308.100143.

Sø, H. U., Postma, D., Lan, V. M., Trang, P. T. K., Kazmierczak, J., Nga, D. V., Pi, K., Koch, C. B., Viet, P. H., Jakobsen, R. (2018). Arsenic in Holocene aquifers of the Red River floodplain, Vietnam: Effects of sediment-water interactions, sediment burial age and groundwater residence time. *Geochim. Cosmochim. Acta*, 225, 192-209. https://doi.org/10.1016/j.gca.2018.01.010.

Steelman, C. M., Klazinga, D. R., Cahill, A. G., Endres, A. L., Parker, B. L. (2017). Monitoring the evolution and migration of a methane gas plume in an unconfined sandy aquifer using time-lapse GPR and ERT. J. Contam. Hydrol., 205, 12–24. https://doi.org/10.1016/j.jconhyd.2017.08.011.

Stolper, D. A., Lawson, M., Davis, C. L., Ferreira, A. A., Santos Neto E. V., Ellis, G. S., Lewan, M. D., Martini, A. M., Tang, Y., Schoell, M., Sessions, A. L., Eiler, J. M. (2014). Gas formation. Formation temperatures of thermogenic and biogenic methane. *Science*. 344(6191) 1500-3. https://doi.org/10.1126/science.1254509.

Stopelli, E., Duyen, V. T., Prommer, H., Glodowska, M., Kappler, A., Schneider, M., Eiche, E., Lightfoot, A. K., Schubert, C. J., Trang, P. K. T., Viet, P. H., Kipfer, R., Winkel, L. H. E., Berg, M. (2021). Carbon and methane cycling in arsenic-contaminated aquifers. *Water Res.*, 200, 117300. https://doi.org/10.1016/j.watres.2021.117300.

Swartz, C. H., Blute, N. K., Badruzzman, B., Ali, A., Brabander, D., Jay, J., Besancon, J., Islam, S., Hemond, H. F., Harvey, C. F. (2004). Mobility of arsenic in a Bangladesh aquifer: Inferences from geochemical

856 profiles, leaching data, and mineralogical characterization. *Geochim. Cosmochim. Acta*, 68(22), 4539–
857 4557. https://doi.org/10.1016/j.gca.2004.04.020.

858 Thullner, M., Fischer, A., Richnow, H. H., Wick, L. Y. (2013). Influence of mass transfer on stable isotope
859 fractionation. *Appl. Microbiol. Biotechnol.*, 97(2), 441–452. https://doi.org/10.1007/s00253-012-
860 4537-7.

861 Bangladesh Bureau of Statistics (BBS) and UNICEF Bangladesh. (2015). Bangladesh multiple indicator
862 cluster survey 2012-2013, ProgotirPathey: Final Report. Bangladesh Bureau of Statistics (BBS) and
863 UNICEF Bangladesh, Dhaka, Bangladesh ISBN: 978-984-8969-21-2.

864 Volanis, D., Kadiyska, T., Galanis, A., Delakas, D., Logotheti, S., Zoumpourlis, V. (2010). Environmental
865 factors and genetic susceptibility promote urinary bladder cancer. *Toxicol. Lett.*, 193(2), 131–137.
866 https://doi.org/10.1016/j.toxlet.2009.12.018.

867 Wasserstein, R.L., Schirm, A.L., Lazar, N.A., 2019. Moving to a world beyond "p < 0.05". *Am. Stat*. 73, 1–
868 19. https://doi.org/10.1080/00031305.2019.1583913.

869 Whiticar, M. J., Faber, E., Schoell, M. (1986). Biogenic methane formation in marine and freshwater
870 environments: CO_2 reduction vs. acetate fermentation-Isotope evidence. *Geochim. Cosmochim. Acta*,
871 50(5), 693–709. https://doi.org/10.1016/0016-7037(86)90346-7.

872 Whiticar, M. J. (1999). Carbon and hydrogen isotope systematics of bacterial formation and oxidation of
873 methane. *Chem. Geol.*, 161. https://doi.org/10.1016/S0009-2541(99)00092-3.

874 Whiticar, M. J. (2020). The biogeochemical methane cycle. In: Hydrocarbons, Oils and Lipids: Diversity,
875 Origin, Chemistry and Fate, 669–746. Cham: Springer International Publishing.
876 https://doi.org/10.1007/978-3-319-90569-3_5.

877 Weiss, R. F. (1970). The solubility of nitrogen, oxygen and argon in water and seawater. *Deep-Sea Research*
878 *and Oceanographic Abstracts*, 17(4), 721–735. https://doi.org/10.1016/0011-7471(70)90037-9.

879 Weiss, R. F. (1974). Carbon dioxide in water and seawater: the solubility of a non-ideal gas. *Mar. Chem.*, 2(3),
880 203–215. https://doi.org/10.1016/0304-4203(74)90015-2.

881 Wu, R., Xu, L., Polya, D.A. (2021) Groundwater arsenic-attributable cardiovascular disease (CVD) mortality
882 risks in India. *Water*. 13(16), 2232. https://doi.org/10.3390/w13162232.

883 Wu, R, Richards LA, Roshan, A., Polya, D.A. (2023) Artificial intelligence modelling to support the
884 groundwater chemistry-dependent selection of groundwater arsenic remediation approaches in
885 Bangladesh. *Water*, 15(20), 3539; https://doi.org/10.3390/w15203539.

886 Xu, L., Mondal, D., Polya, D.A. (2020) Positive association of cardiovascular disease (CVD) with chronic
887 exposure to drinking water arsenic at concentration below the WHO Provisional Guideline Value: A
888 systematic review and meta-analysis. *Int. J. Env. Res. Public Health*, 17(7), Art. No. 2536.
889 https://doi.org/10.3390/ijerph17072536.

890 Yamamoto, S., Alcauskas, J. B., Crozier, T. E. (1976). Solubility of methane in distilled water and seawater. *J.*
891 *Chem. Eng. Data*, 21(1), 78–80. https://doi.org/10.1021/je60068a029.